USC–SIPI REPORT #287

Radar Clutter Modeling Using Stable Distributions

by

Xinyu Ma and Chrysostomos L. Nikias

September 1995

Signal and Image Processing Institute
UNIVERSITY OF SOUTHERN CALIFORNIA
Department of Electrical Engineering-Systems
3740 McClintock Avenue, Room 404
Los Angeles, CA 90089-2564 U.S.A.

Radar Clutter Modeling Using Stable Distributions

Xinyu Ma (Student Member) and Chrysostomos L. Nikias (Fellow, IEEE)

Signal & Image Processing Institute

Department of Electrical Engineering-Systems

University of Southern California

Los Angeles, CA 90089-2564

Tel: (213)740-2218 Fax: (213)740-4651

email: xma@sipi.usc.edu

Abstract

We present new methods for parameter estimation in the impulsive signal environments, which are modeled as symmetric alpha-stable (SαS) processes. There are two parts in this report. In the first part, we present several methods for estimation of parameters (the characteristic exponent α and the dispersion γ) of a SαS process. In the second part, we apply the estimation algorithms to radar clutter modeling. It is shown that SαS can characterize the clutter environments accurately.

1 Introduction

Stable distributions are important for statistical signal processing. By the Generalized Central Limit Theorem, they are the *only* class of distributions that can be the limiting distributions for sums of iid random variables with finite or infinite variances. Familiar members of the family are Gaussian ($\alpha = 2$) and Cauchy ($\alpha = 1$) distributions. Many signal/noise processes are impulsive in nature and can be best modeled as α-stable processes [3]. Unlike most statistical models, the α-stable distributions (except Gaussian) have infinite second- or higher-order moments. With this unique property, many fundamental theories in signal processing have to be modified. For a comprehensive introduction of α-stable distributions and their applications to signal processing, see the first monograph by C. L. Nikias and M. Shao [2]. An alternative tool is the fractional lower-order moments (FLOM) and covariations.

Radar clutter is usually highly impulsive. Stable distributions are attractive candidate for modeling of such environments. In the second part of this report, we apply the proposed parameter estimation algorithm to clutter modeling using SαS distributions. Comparison has been made against the Gaussian model.

2 Estimation of the Characteristic Exponent and the Dispersion

2.1 Fractional Lower-Order Moments: Positive-Order and Negative-Order

It has been shown that fractional lower-order moments $\mathbf{E}\{|X|^p\}$ for a real, zero-location SαS random variable X are finite for $-1 < p < \alpha$ [1]. More specifically,

$$\mathbf{E}(|X|^p) = \frac{2^{p+1}\Gamma(\frac{p+1}{2})\Gamma(-p/\alpha)}{\alpha\sqrt{\pi}\Gamma(-p/2)}\gamma^{p/\alpha}, \text{ for } -1 < p < \alpha. \tag{1}$$

When X is an n dimensional spherically symmetric SαS random variable, a similar expression is [5]:

$$\mathbf{E}(|X|^p) = 2^p \frac{\Gamma(\frac{p+n}{2})\Gamma(1-\frac{p}{\alpha})}{\Gamma(1-\frac{p}{2})\Gamma(\frac{n}{2})} \gamma^{p/\alpha}, \text{ for } \quad -n < p < \alpha. \tag{2}$$

Especially, when $n = 2$, X is then called *isotropic complex* SαS random variable, we have:

$$\mathbf{E}(|X|^p) = C_2(p,\alpha)\gamma^{p/\alpha}, \text{ for } \quad -2 < p < \alpha, \tag{3}$$

where $C_2(p,\alpha) = 2^p \frac{\Gamma(1+\frac{p}{2})\Gamma(1-\frac{p}{\alpha})}{\Gamma(1-\frac{p}{2})}$.

An immediate application of the negative-order moments is for estimating the characteristic exponent α and the dispersion γ of SαS random processes. If X is a real SαS random variable, with zero location parameter, then its positive order FLOM is given by $\mathbf{E}(|X|^p) = C_1(p,\alpha)\gamma^{p/\alpha}$, for $0 < p < \alpha$; and its negative order FLOM is given by $\mathbf{E}(|X|^q) = C_1(q,\alpha)\gamma^{q/\alpha}$, for $-1 < q < 0$. Choosing $p = -q$ (since $-1 < q < 0$, then $0 < p < \min(\alpha, 1)$ such that both positive- and negative-order moments are finite), then we have:

$$\mathbf{E}(|X|^p)\mathbf{E}(|X|^{-p}) = \frac{2\tan(p\pi/2)}{\alpha \sin(p\pi/\alpha)}, \tag{4}$$

i.e., α can be found by the solving the following sinc function:

$$\text{sinc}(\frac{p\pi}{\alpha}) = \frac{\sin(\frac{p\pi}{\alpha})}{(\frac{p\pi}{\alpha})} = \frac{2\tan(p\pi/2)}{p\pi\mathbf{E}(|X|^p)\mathbf{E}(|X|^{-p})}, 0 < p < \min(\alpha, 1). \tag{5}$$

The above equation does not involve γ. Once α is estimated, γ can be solved by:

$$\gamma = \left(\frac{\alpha\pi\mathbf{E}(|X|^p)}{2\Gamma(1+p)\Gamma(-p/\alpha)\sin(-p\pi/2)} \right)^{\alpha/p}. \tag{6}$$

2.2 Parameter Estimation with $\log|\text{S}\alpha\text{S}|$ process

Assuming X is one-dimensional SαS random variable, we have shown its p^{th}-order moment is:

$$\mathbf{E}\{|X|^p\} = \frac{2^p\Gamma(\frac{p+1}{2})\Gamma(1-p/\alpha)}{\sqrt{\pi}\Gamma(1-p/2)}\gamma^{p/\alpha}, \forall p : -1 < p < \alpha. \tag{7}$$

We can rewrite $\mathbf{E}(|X|^p)$ as $\mathbf{E}(e^{p\log|X|})$, (note that $\log|X|$ is bounded because the pdf of X: $f(x)$ is bounded at $x = 0$, i.e., the probability of $x = 0$ is 0). Define a new random variable $Y = \log|X|$, therefore:

$$\mathbf{E}(|X|^p) = \mathbf{E}(e^{p\log|X|}) = \mathbf{E}(e^{pY}). \tag{8}$$

Notice the last term in the above equation $\mathbf{E}(e^{pY})$ is the moment-generating function of Y, we can expand it into a power series:

$$\mathbf{E}(e^{pY}) = \sum_{k=0}^{\infty} \mathbf{E}(Y^k)\frac{p^k}{k!}. \tag{9}$$

On the other hand,

$$\mathbf{E}(|X|^p) = \mathbf{E}(e^{pY}) = \frac{2^p\Gamma(\frac{p+1}{2})\Gamma(1-p/\alpha)}{\sqrt{\pi}\Gamma(1-p/2)}\gamma^{p/\alpha}, \forall p: -1 < p < \alpha. \tag{10}$$

Therefore, moments of Y of any order must be finite and they satisfy:

$$\mathbf{E}(Y^k) = \frac{d^k}{dp^k}\left(\frac{2^p\Gamma(\frac{p+1}{2})\Gamma(1-p/\alpha)}{\sqrt{\pi}\Gamma(1-p/2)}\gamma^{p/\alpha}\right)|_{p=0}. \tag{11}$$

Simplifying the above equation, we have:

$$\mathbf{E}(Y) = \mathbf{C}_e(\frac{1}{\alpha} - 1) + \frac{1}{\alpha}\log\gamma, \tag{12}$$

where $\mathbf{C}_e = 0.57721566\cdots$ is the Euler constant, α is the characteristic exponent, γ is the dispersion, and

$$\mathbf{Var}(Y) = \mathbf{E}\{(Y - \mathbf{E}\{Y\})^2\} = \frac{\pi^2}{6}\left(\frac{1}{\alpha^2} + \frac{1}{2}\right), \tag{13}$$

$$\mathbf{E}\{(Y - \mathbf{E}\{Y\})^3\} = 2\zeta(3)\left(\frac{1}{\alpha^3} - 1\right), \tag{14}$$

where $\zeta(\cdot)$ is the Riemann Zeta function, and $\zeta(3)$ is a constant: $\zeta(3) = 1.2020569\cdots$.

$$\mathbf{E}\{(Y - \mathbf{E}\{Y\})^4\} = \pi^4\left(\frac{3}{20\alpha^4} + \frac{1}{12\alpha^2} + \frac{19}{240}\right) \tag{15}$$

Order Moment of Y	Second-Order	Third-Order	Fourth-Order
$\hat{\alpha}$	1.5139 (0.1167)	1.4837 (0.2578)	1.3564 (0.3226)
$\hat{\gamma}$	1.0195 (0.0909)	1.0079 (0.1032)	0.9549 (0.1365)

Table 1: Estimator Performance v.s. Order of Moment of Y.

The higher-order moments of Y always exist and from the second-order moment and above, the equations only involve α. This property provides a simple method to estimate the parameters α and γ of a SαS random variable. Since we can estimate the mean and variance of Y by:

$$\bar{Y} = \frac{\sum_{i=1}^{N} Y_i}{N}, \quad \hat{\sigma}_Y^2 = \frac{\sum_{i=1}^{N}(Y_i - \bar{Y})^2}{N-1}, \tag{16}$$

where N is the number of samples and Y_i are iid observations, then by solving Eq.(13), we can obtain an estimate of α and substitute into Eq.(12), we can get an estimate of γ. The $\log|\text{S}\alpha\text{S}|$ process was first introduced by Zolotarev [4].

We can also use higher-order moments of Y to estimate α, but it is known that the variance of the estimator of higher-order moments tends to increase as the order goes higher. Table 1 is a comparison of the results obtained by using different orders of moments. The true values for the parameters are $\alpha = 1.5$ and $\gamma = 1.0$. Y is the $\log|\text{S}\alpha\text{S}|$ process, Sample size is 1000, and the experiment is repeated 1000 times independently. As we can see from Table 1, the standard deviations of the estimators (α-estimator and γ-estimator) increase as the order of the moment of Y increases.

Table 2 lists the comparison of the $\log|\text{S}\alpha\text{S}|$ approach with the negative-order moment method. X is the standard SαS random variable with $\alpha = 1.5$ and $Y = \log|X|$. We chose $p = 0.2$ in the negative-order moment method. The experiment was repeated 1000 times

Estimation Method	log |SαS| Approach	Negative-Order Moment
$\hat{\alpha}$	1.4969	1.5027
	(0.0522)	(0.0536)
$\hat{\gamma}$	0.9989	1.0023
	(0.0385)	(0.0423)

Table 2: Performance comparison of the log |SαS| approach v.s. the negative-order moment method.

independently with 5000 iid samples.

Table 2 shows that these two methods have similar performance. But the advantages of the log |SαS| approach are:

1. It gives explicit closed form expressions of the unknown parameters, whereas in the negative-order moment method, α is involved in the sinc function, which does not have a closed form expression.

2. The estimates of the parameters are completely determined by the samples collected, whereas in the negative-order moment method, the estimation results are also affected by the value p we choose, and the choice of p is often empirical.

It is worth noticing that the above proposed estimators are not the optimal ones as the Maximum-Likelihood Estimators. However, MLEs do not have such simple closed form expressions and the estimates are obtained through solving nonlinear optimization problems. Therefore, its application in real-time SαS signal processing is limited.

Similarly, if X is an isotropic complex SαS random variable then its pth order moment satisfies (3). The log |SαS| approach yields:

$$\mathbf{E}(Y) = \mathbf{C}_e(\frac{1}{\alpha} - 1) + \log 2 + \frac{1}{\alpha}\log\gamma, \tag{17}$$

Sample Size	1000	5000	10000
$\hat{\alpha}$	1.2036	1.1997	1.1987
(true $\alpha = 1.2$)	(0.0391)	(0.0184)	(0.0118)
$\hat{\gamma}$	1.0037	1.0008	1.0026
(true $\gamma = 1$)	(0.0359)	(0.0162)	(0.0136)

Table 3: Performance of the log |SαS| Estimator for the isotropic complex SαS process.

$$\mathbf{Var}(Y) = \frac{\pi^2}{6\alpha^2}, \tag{18}$$

where $Y = \log|X|$, (17) and (18) can be used to estimate α and γ of an isotropic complex SαS process. Table 3 shows the average and standard deviation values (in parentheses) of Monte-Carlo simulation results (see Appendix A for the isotropic complex SαS random number generator). The experiment was repeated 100 times independently. The sample size ranges from 1000 to 10,000.

3 Radar Clutter Modeling with Stable Laws

Radar clutter processes are highly impulsive. The empirical distribution densities of such processes are usually algebraically decaying. This suggests that stable laws may characterize such environments accurately.

This section includes the experiments we conducted on SαS modeling of radar clutters using the real data files, which are from the Mountaintop Data Package tape. The clutter data set contains measured monostatic clutter using Radar Surveillance Technology Experimental Radar (RSTER). The data consist of four files: cm435al.bfr, cm435bl.bfr, cm435cl.bfr, and ncal435a.bfr. These data files were collected on August 27, 1993 as part of the Clutter Map Multi-Frequency Experiment. The data are unequalized I/Q data and the waveform employed was a 5 μSec pulsed CW signal at 435 MHz. File cm435al covers from 3.5 to 43.5 nmi in range. File cm435bl covers from 40 to 80 nmi in range. File cm435cl covers from 75 to 115 nmi in range. All of these files have enough CPIs to cover 360 degrees in azimuth. The file ncal435a contains the system noise. In our comprehensive study, we conduct our experiments in 24 different azimuth with 15 degrees interval. Experiments with the actual raw data are performed with the I/Q clutter data on Sensor # 1 (There are 14 sensors in the linear array). In the SαS model, we assume that the I/Q data are *isotropic complex* The parameters (characteristic exponent α and dispersion γ) are first estimated using (17) and (18), then estimated by amplitude probability density (APD) curve fitting through exhaustive search. On the other hand, in the Gaussian model, the variance is estimated by taking standard deviation of the data. The samples are assumed to be i.i.d. and for convenience, the data have been scaled by 10^5. In the following figures, we show the I/Q data time series, estimated parameters and APD comparison along azimuth at 0°, 15°, 30°, 45°, 60°, 75°, 90°, 105°, 120°, 135°, 150°, 165°, 180°, 195°, 210°, 225°, 240°, 255°, 270°, 285°, 300°, 315°, 330°, 345°.

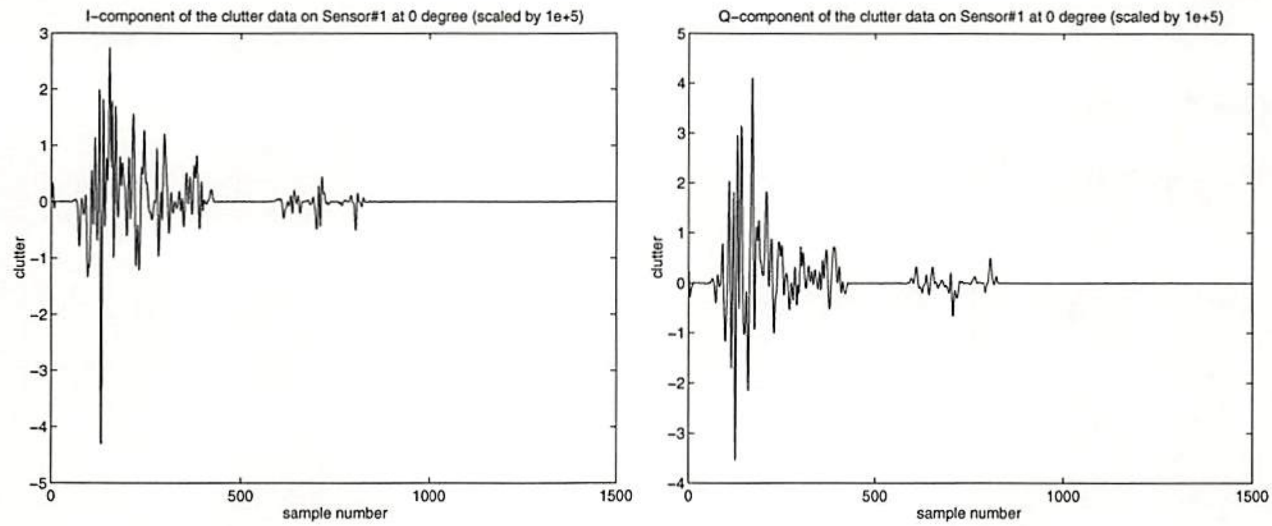

Figure 1: Measured I/Q-components of radar clutter: Azimuth: $0°$, estimated mean: $0.0217 + j0.05$, estimated α: 1.1222, γ: 0.0395.

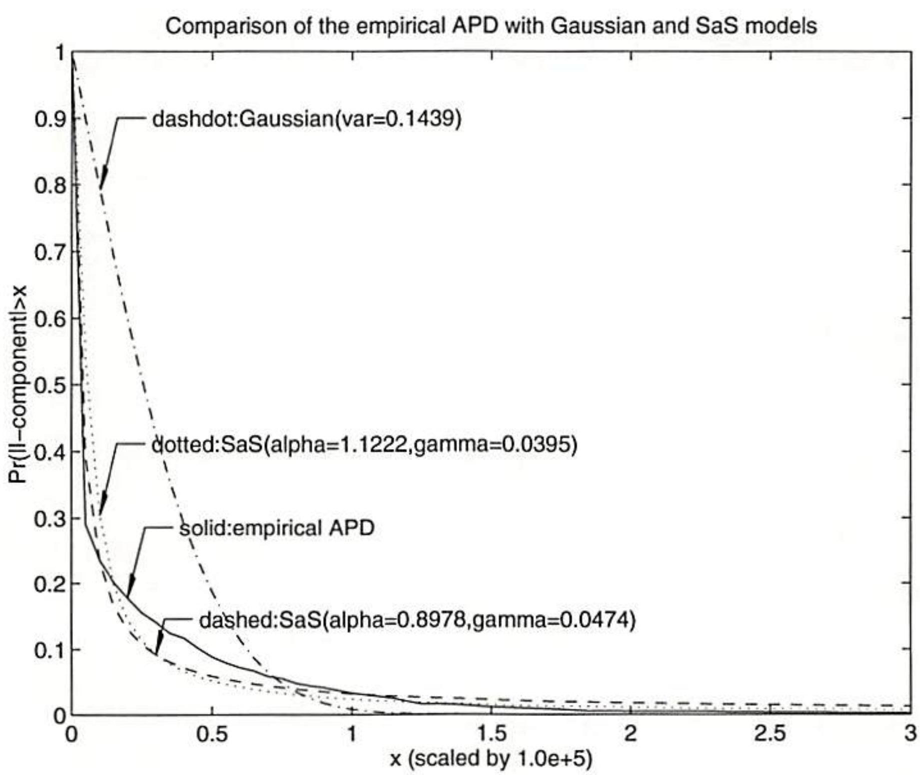

Figure 2: Comparison of the empirical, SαS, and Gaussian amplitude probability distributions

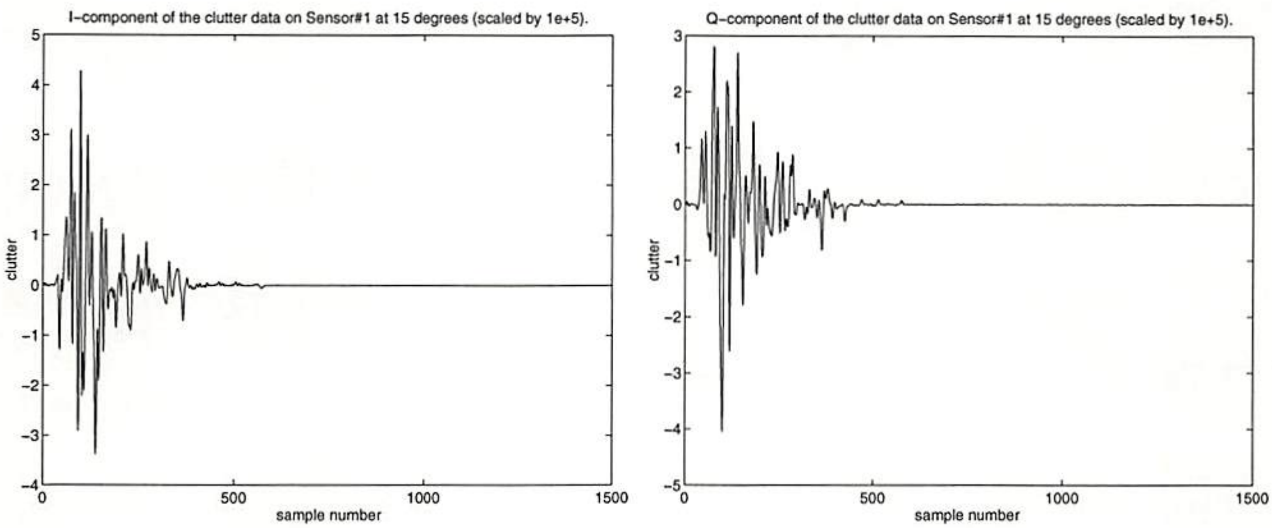

Figure 3: Measured I/Q-components of radar clutter: Azimuth: 15°, estimated mean: $0.0043 + j0.0099$, estimated α: 0.7318, γ: 0.0413.

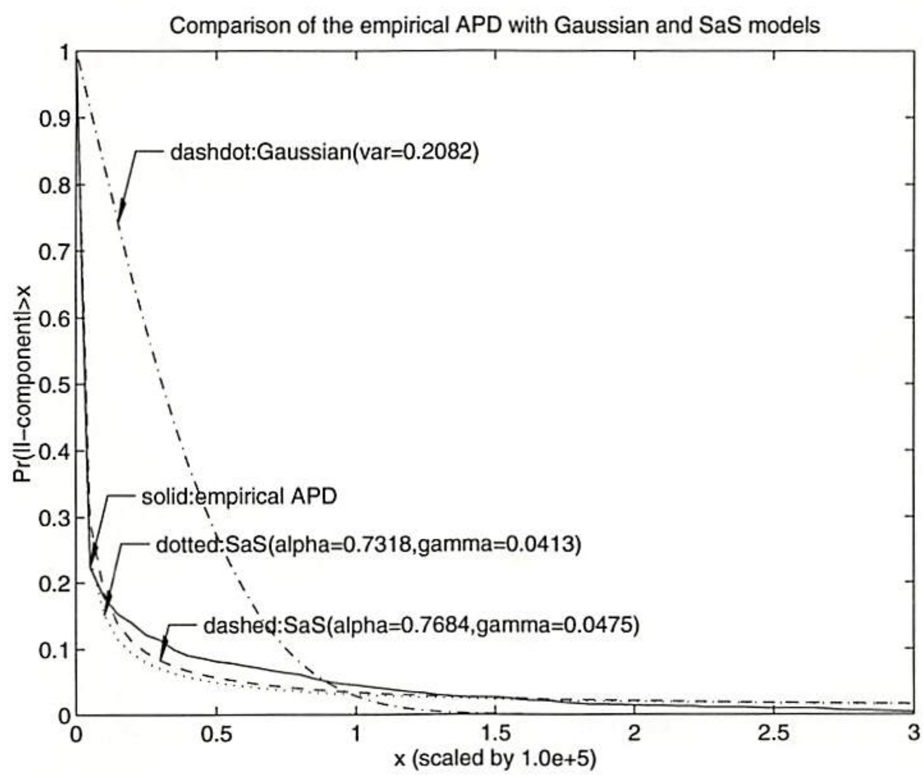

Figure 4: Comparison of the empirical, SαS, and Gaussian amplitude probability distributions

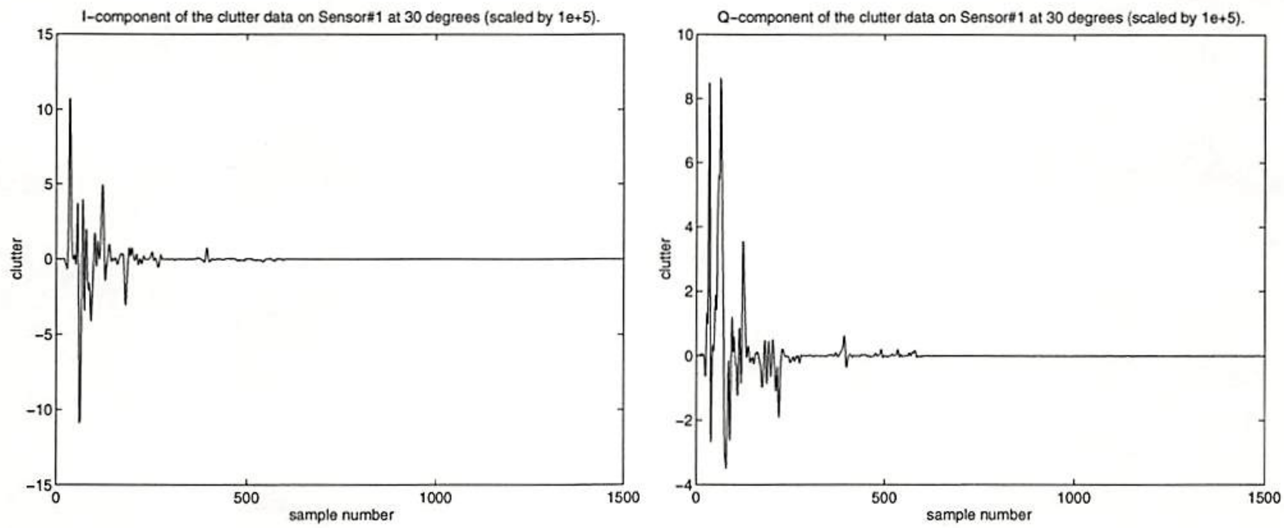

Figure 5: Measured I/Q-components of radar clutter: Azimuth: 30°, estimated mean: $0.001 + j0.0667$, estimated α: 1.164, γ: 0.0351.

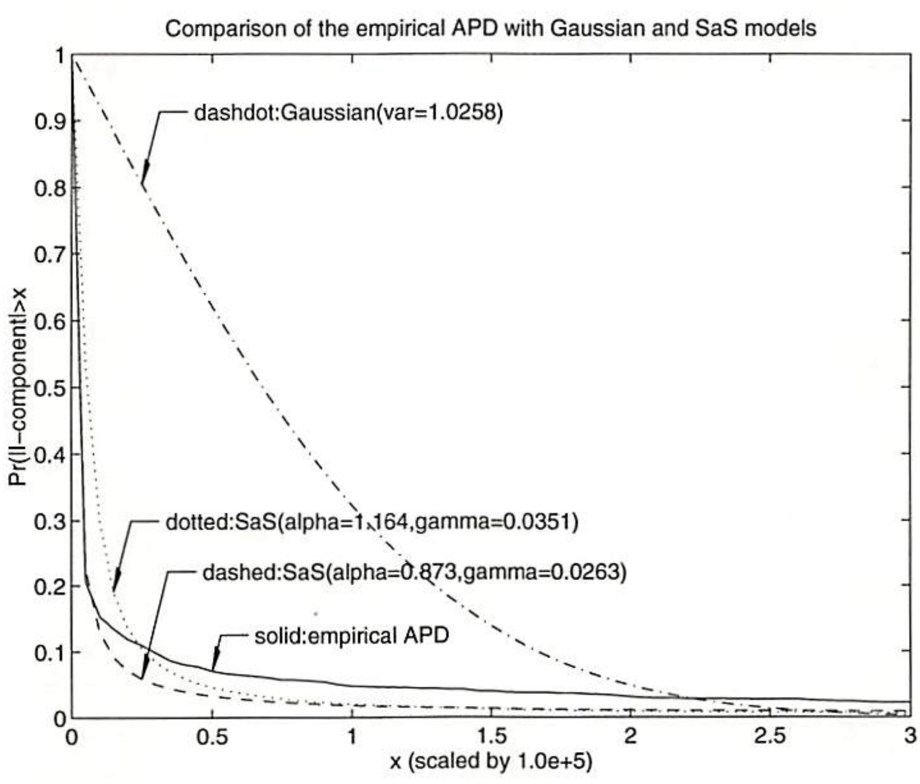

Figure 6: Comparison of the empirical, SαS, and Gaussian amplitude probability distributions

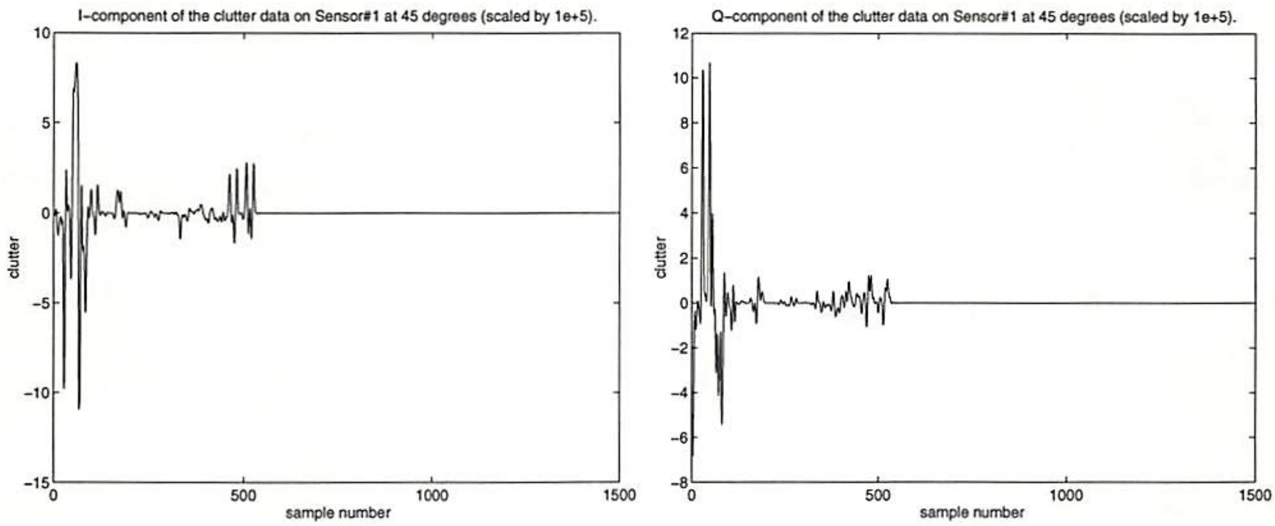

Figure 7: Measured I/Q-components of radar clutter: Azimuth: 45°, estimated mean: $-0.0121 + j0.0247$, estimated α: 0.8301, γ: 0.0537.

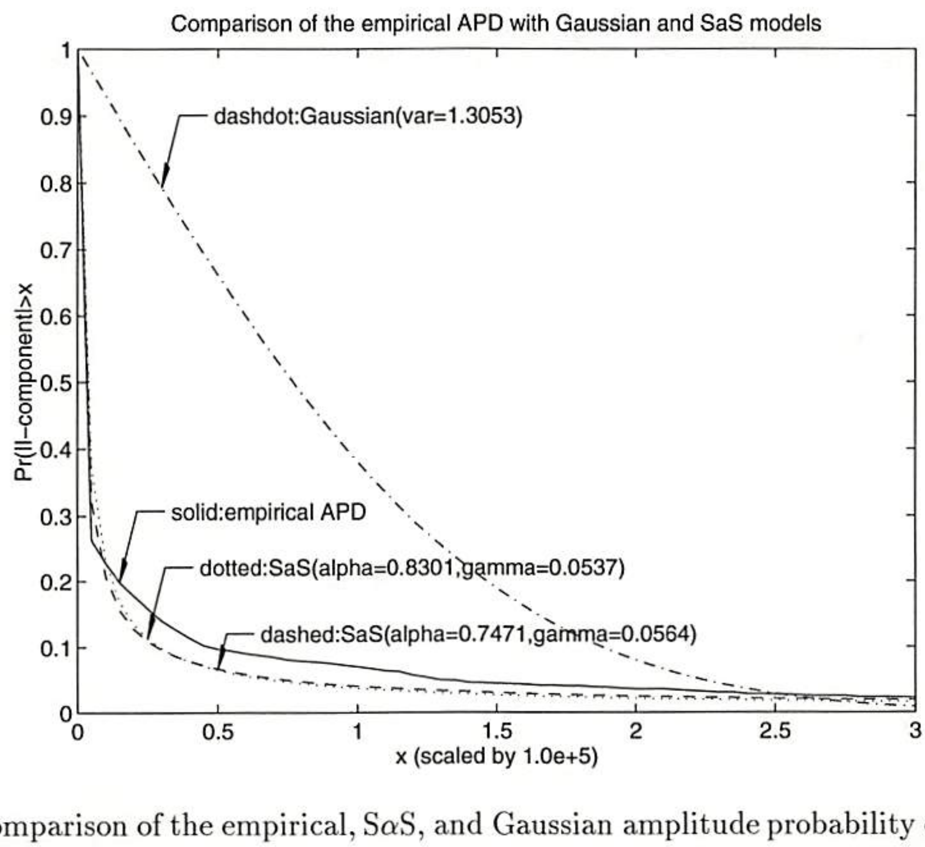

Figure 8: Comparison of the empirical, SαS, and Gaussian amplitude probability distributions

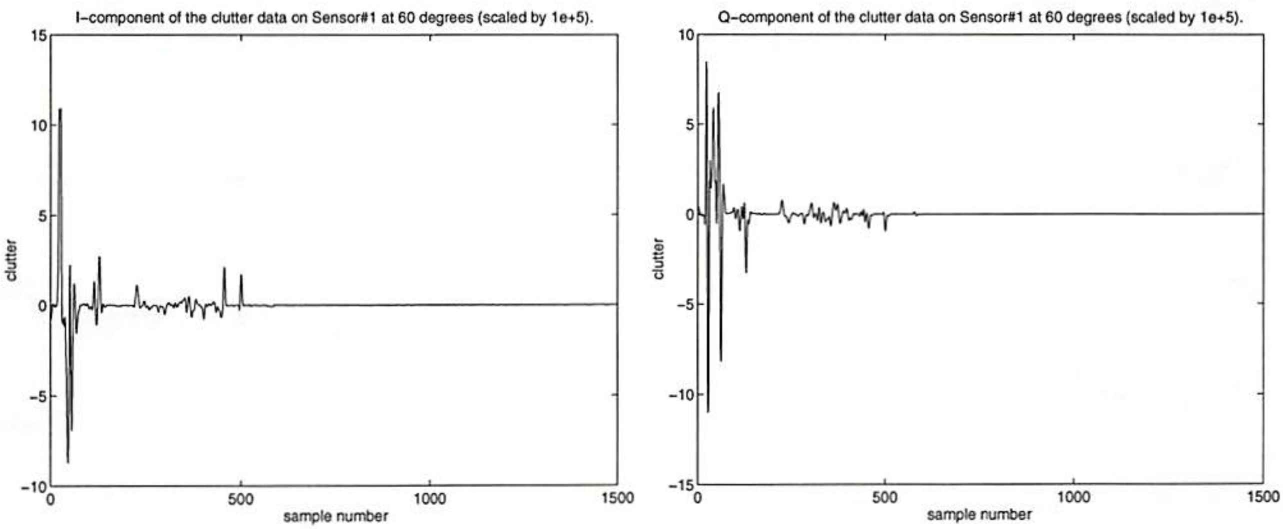

Figure 9: Measured I/Q-components of radar clutter: Azimuth: 60°, estimated mean: $0.0051 + j0.005$, estimated α: 0.6886, γ: 0.0394.

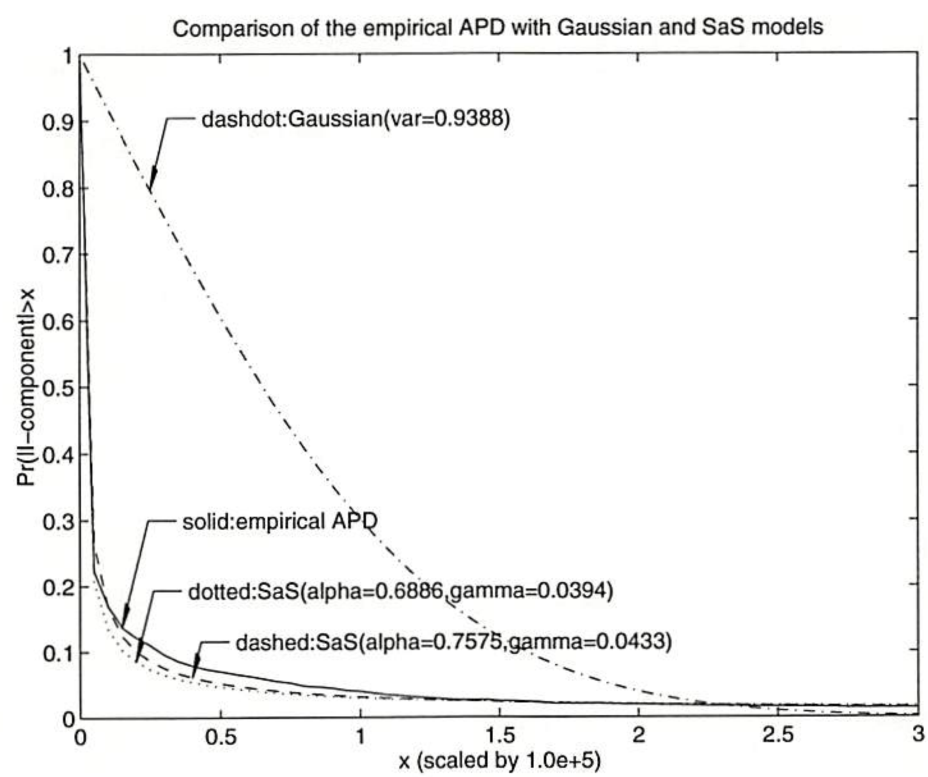

Figure 10: Comparison of the empirical, SαS, and Gaussian amplitude probability distributions

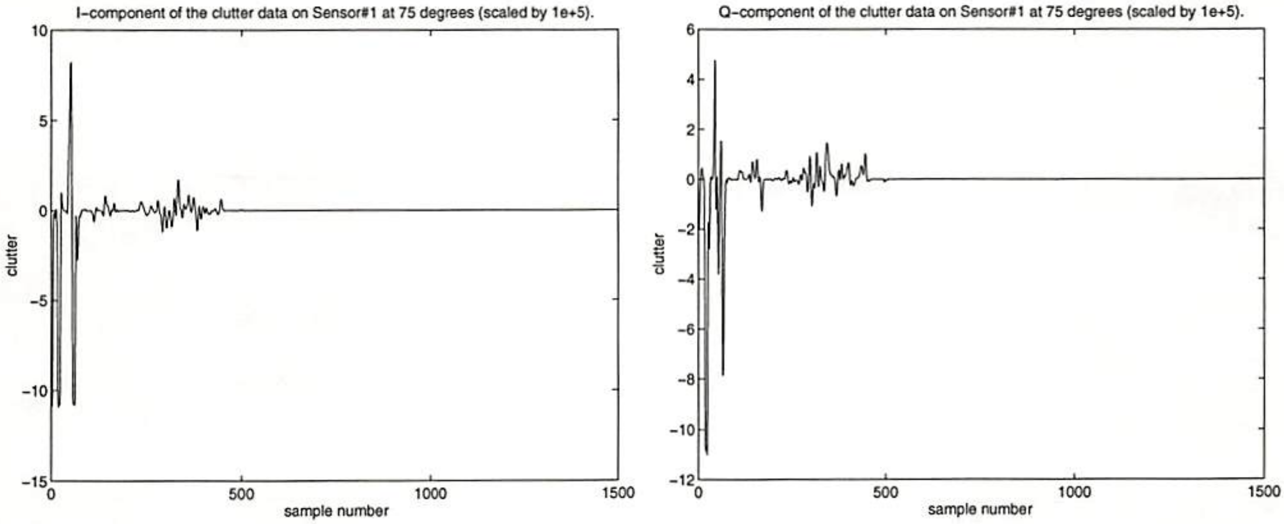

Figure 11: Measured I/Q-components of radar clutter: Azimuth: 75°, estimated mean: $-0.1138 - \jmath 0.0687$, estimated α: 1.4621, γ: 0.041.

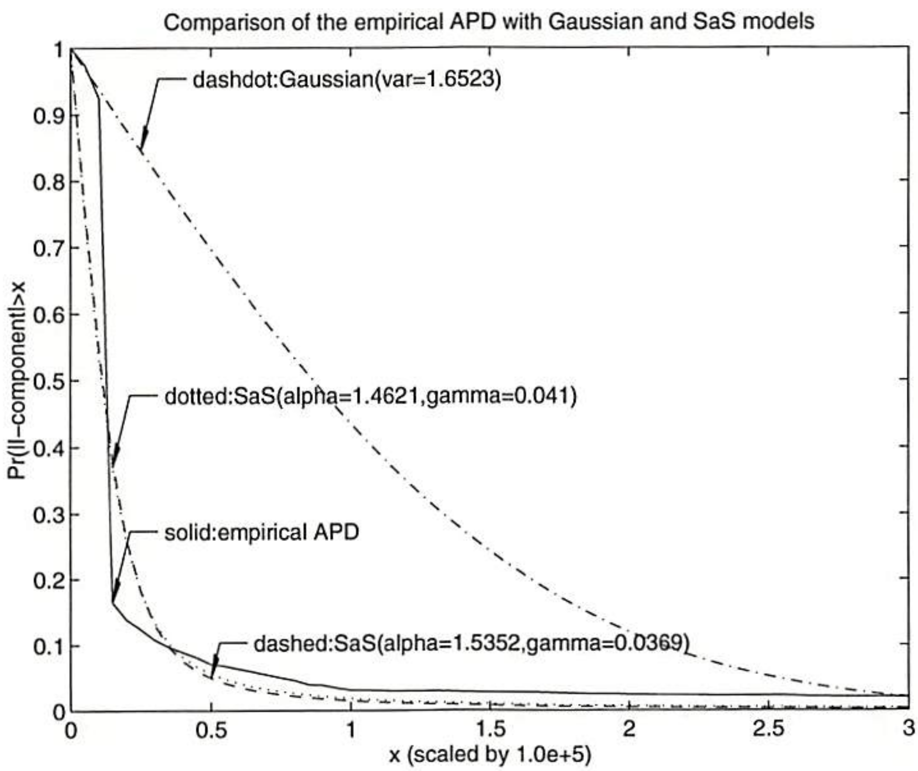

Figure 12: Comparison of the empirical, SαS, and Gaussian amplitude probability distributions

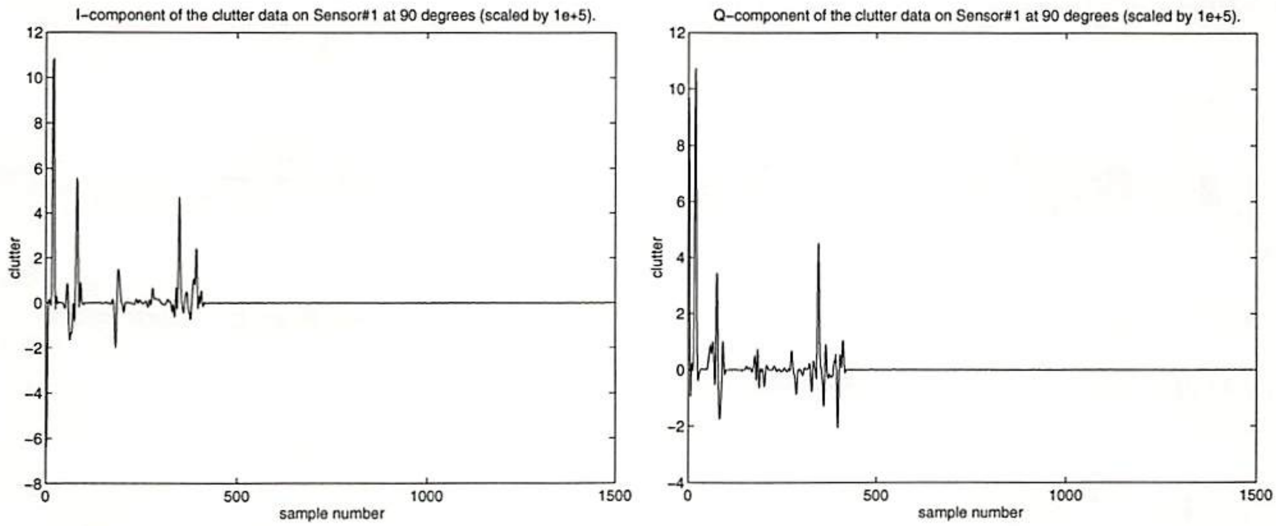

Figure 13: Measured I/Q-components of radar clutter: Azimuth: 90°, estimated mean: $0.0731 + j0.0793$, estimated α: 1.5375, γ: 0.0244.

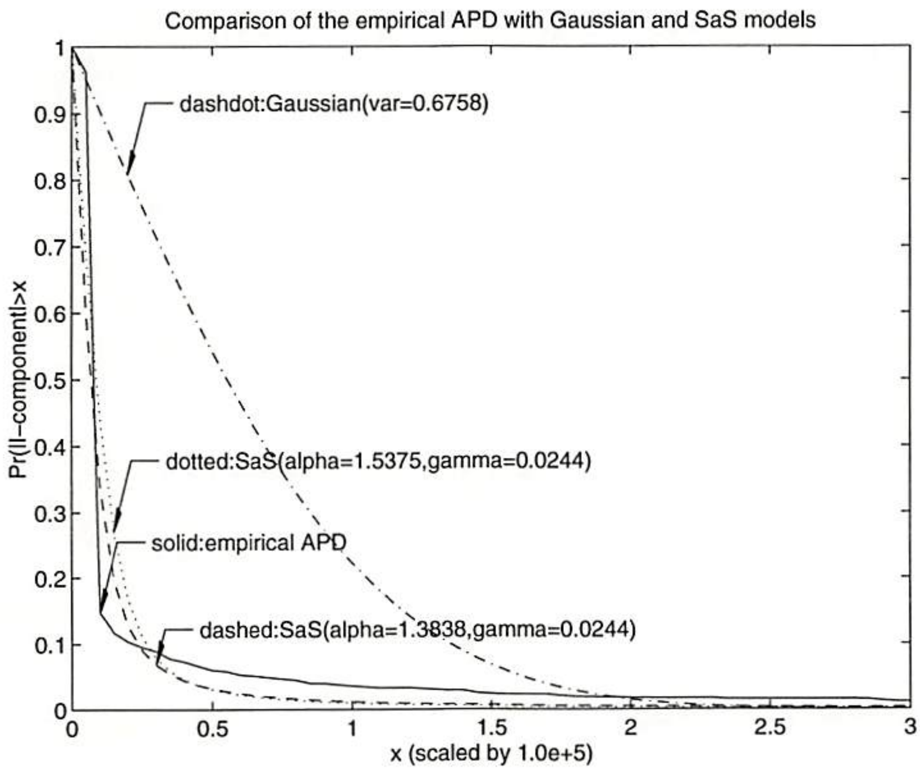

Figure 14: Comparison of the empirical, SαS, and Gaussian amplitude probability distributions

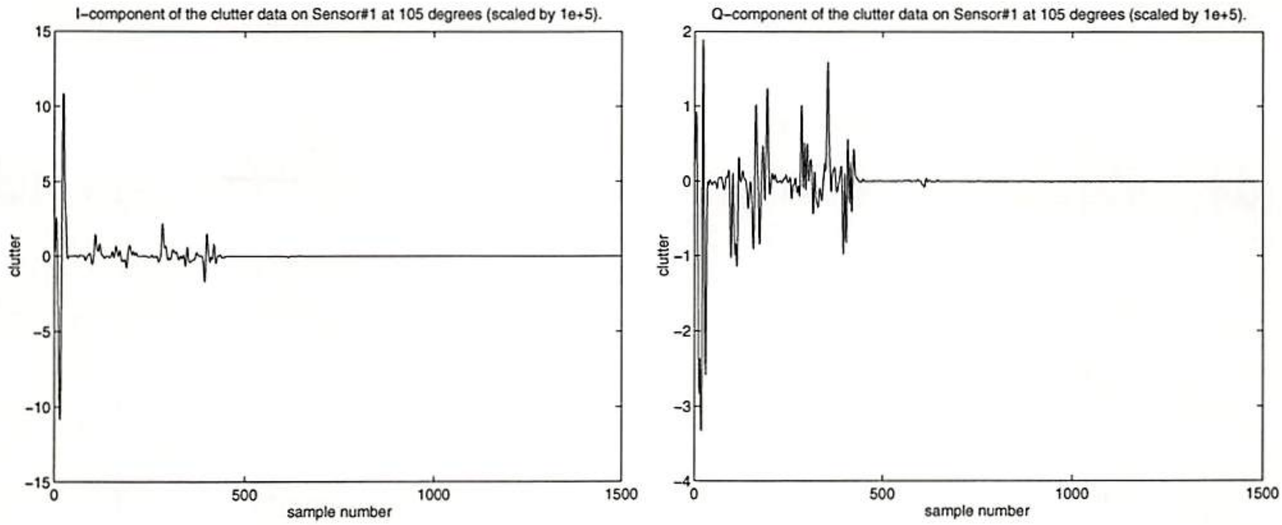

Figure 15: Measured I/Q-components of radar clutter: Azimuth: 105°, estimated mean: $0.028 - j0.0241$, estimated α: 1.1045, γ: 0.0249.

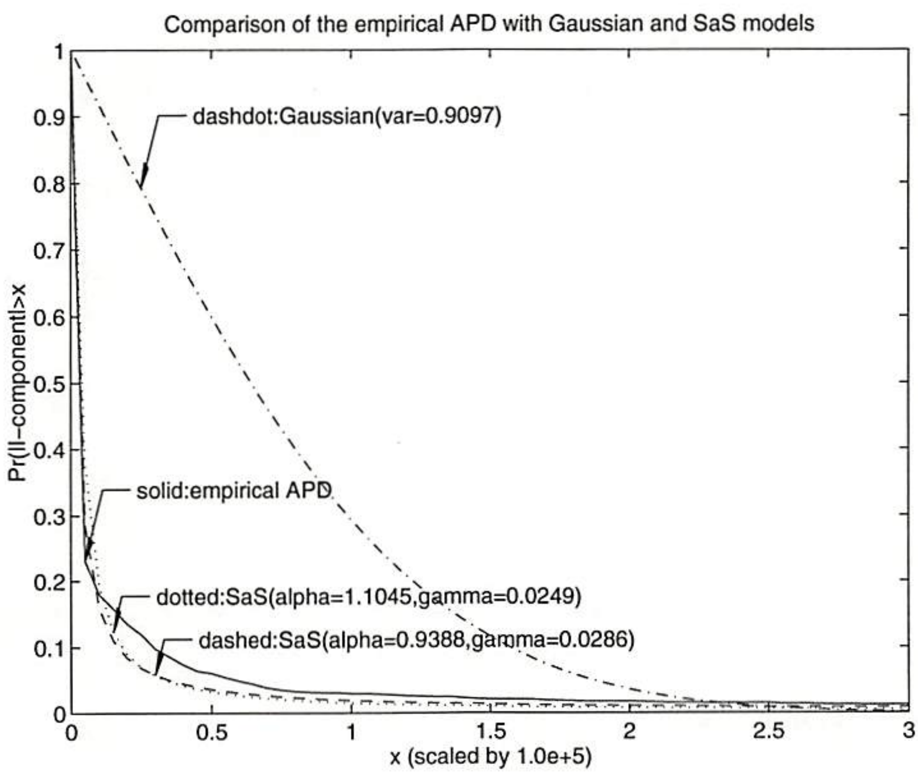

Figure 16: Comparison of the empirical, SαS, and Gaussian amplitude probability distributions

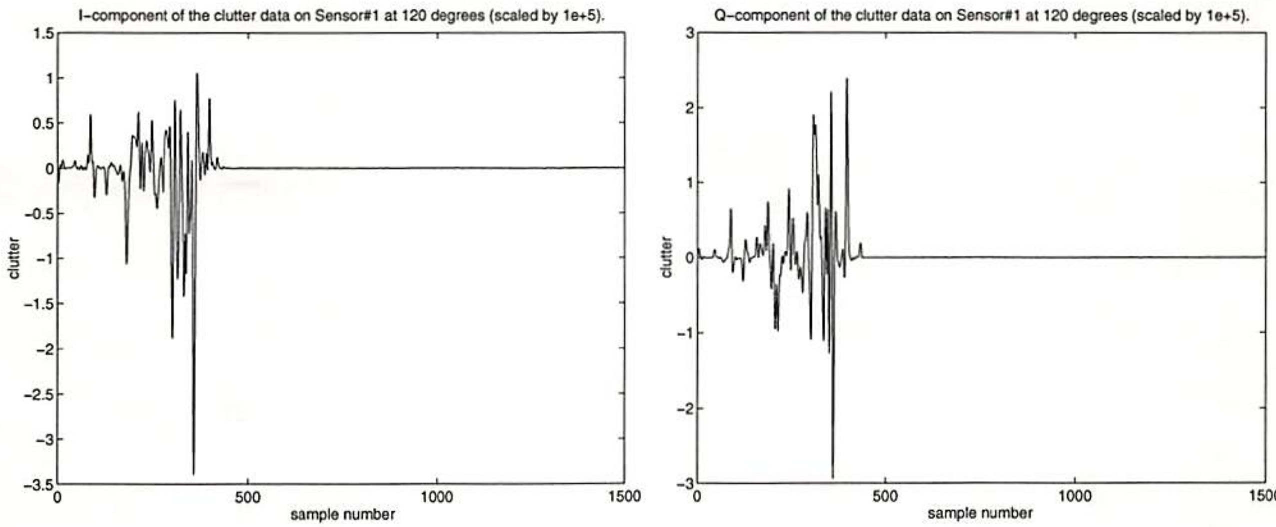

Figure 17: Measured I/Q-components of radar clutter: Azimuth: 120°, estimated mean: $-0.0199 + j0.0215$, estimated α: 1.1314, γ: 0.0171.

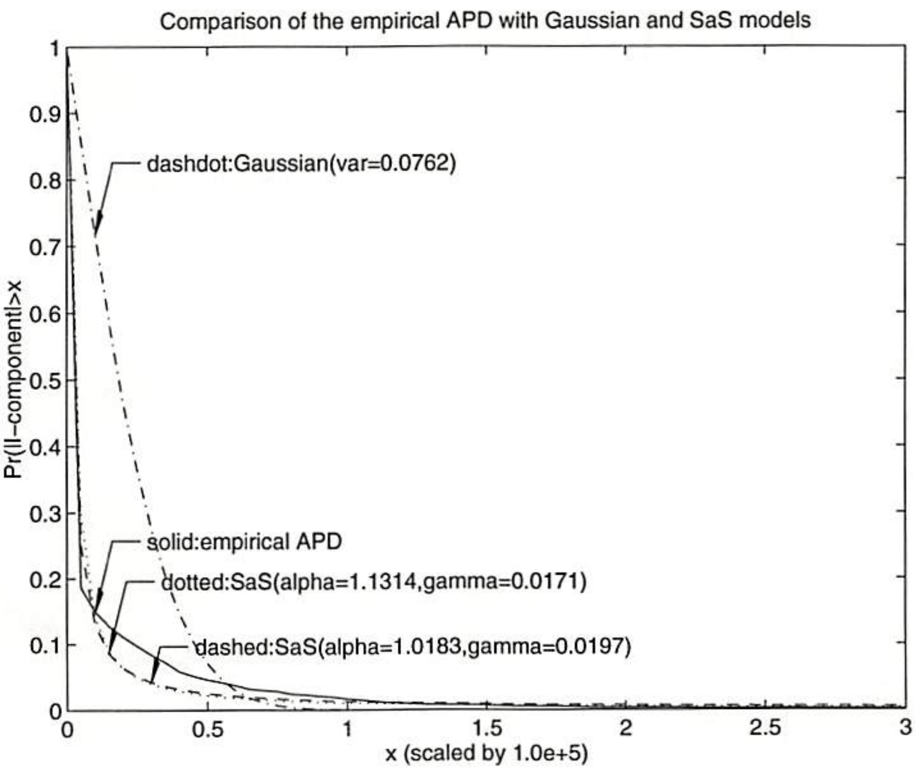

Figure 18: Comparison of the empirical, SαS, and Gaussian amplitude probability distributions

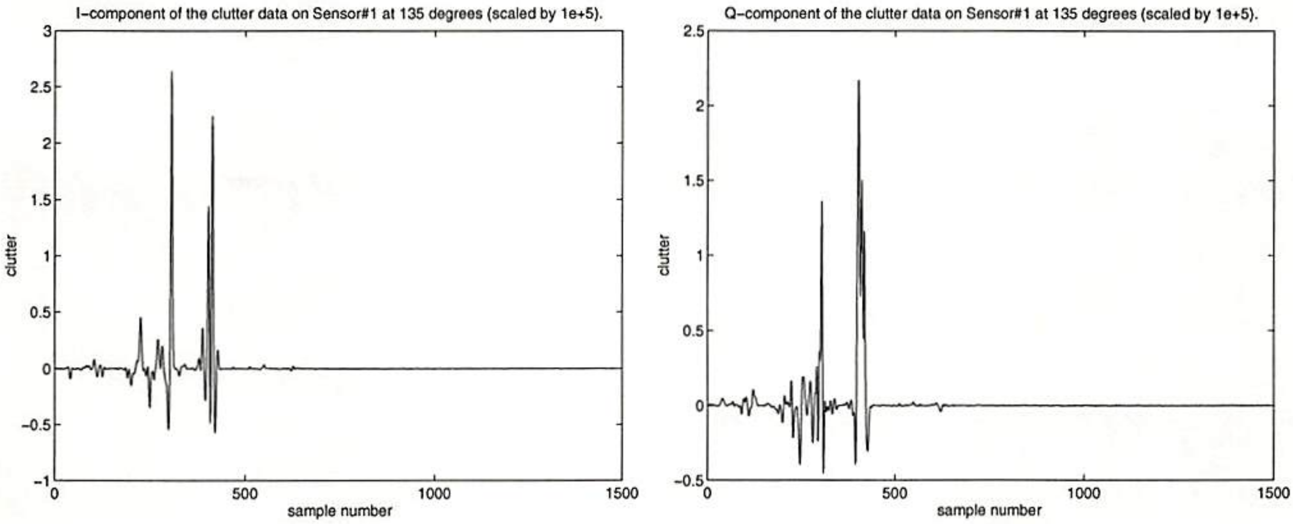

Figure 19: Measured I/Q-components of radar clutter: Azimuth: 135°, estimated mean: $0.0191 + j0.0194$, estimated α: 1.5358, γ: 0.0028.

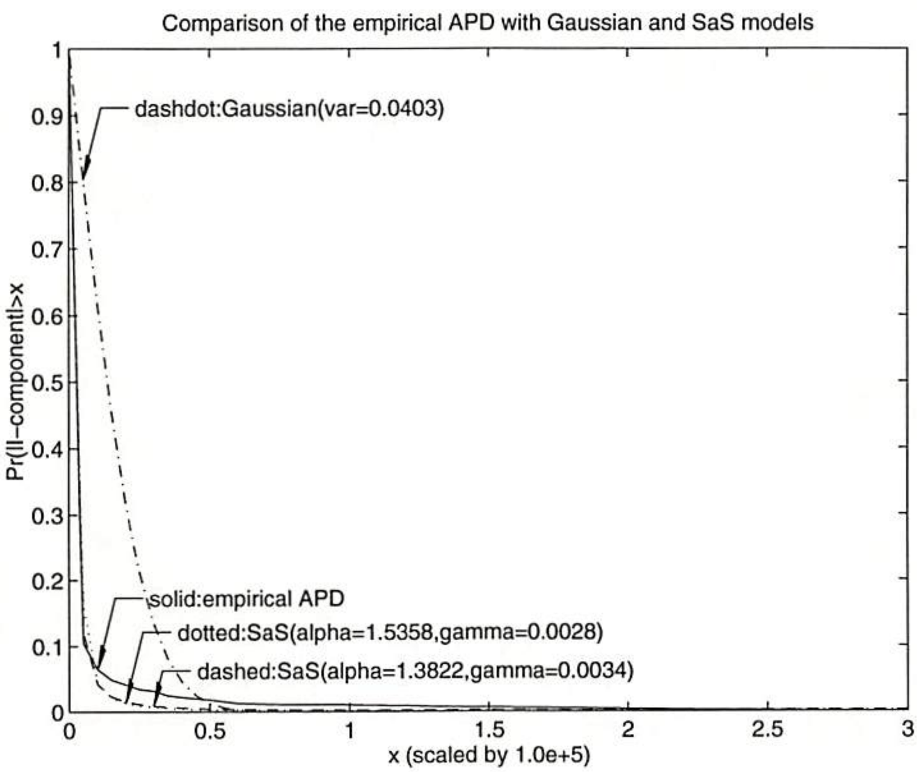

Figure 20: Comparison of the empirical, SαS, and Gaussian amplitude probability distributions

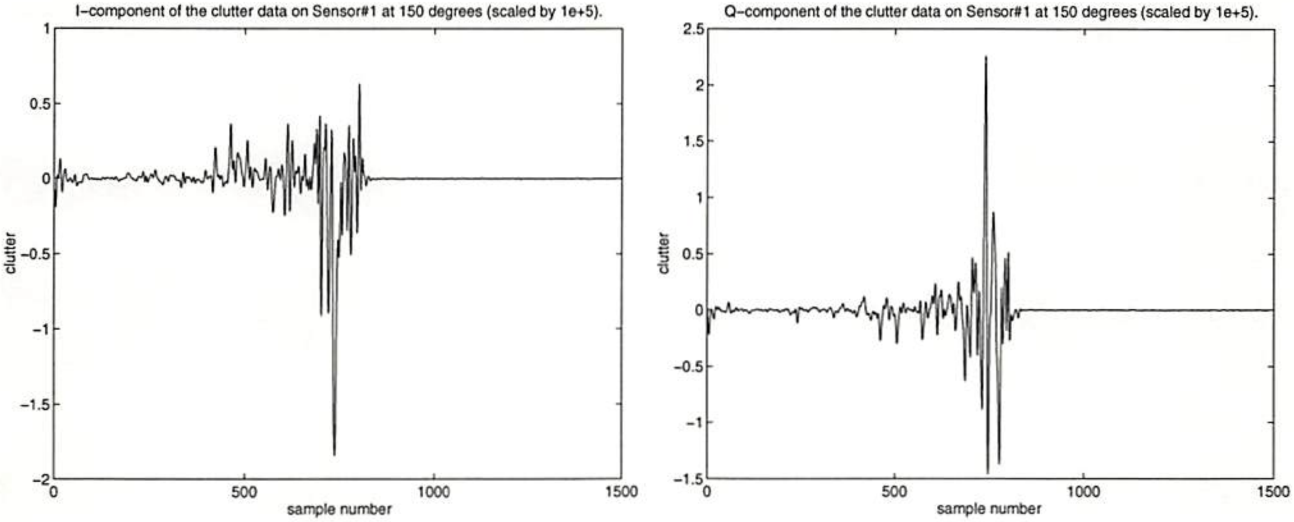

Figure 21: Measured I/Q-components of radar clutter: Azimuth: 150°, estimated mean: $-0.0102 - j0.0043$, estimated α: 0.9783, γ: 0.0144.

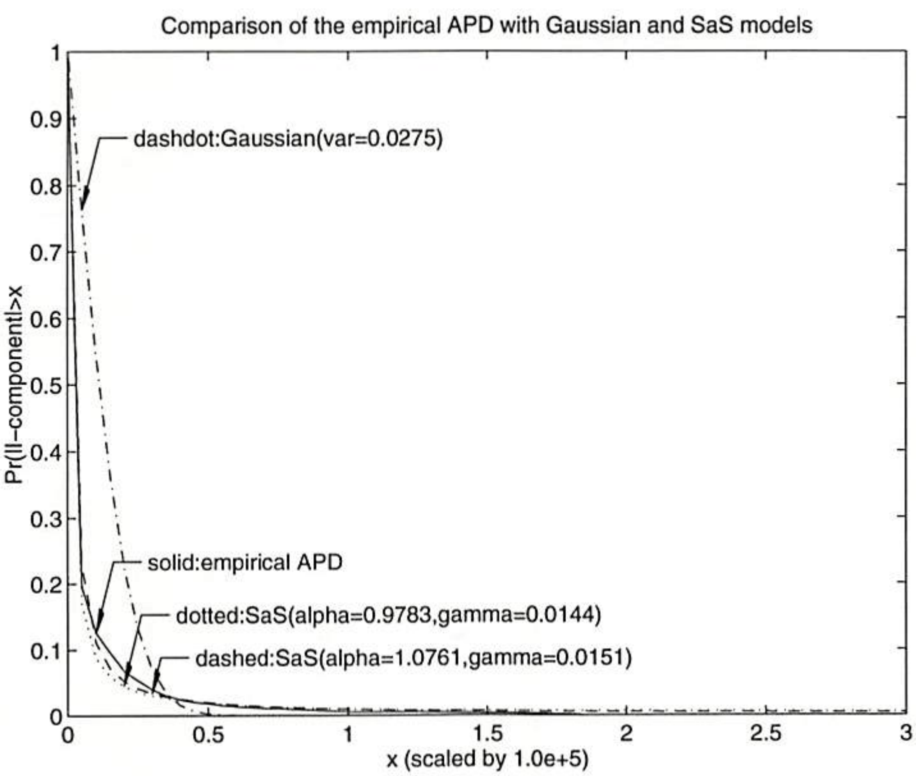

Figure 22: Comparison of the empirical, SαS, and Gaussian amplitude probability distributions

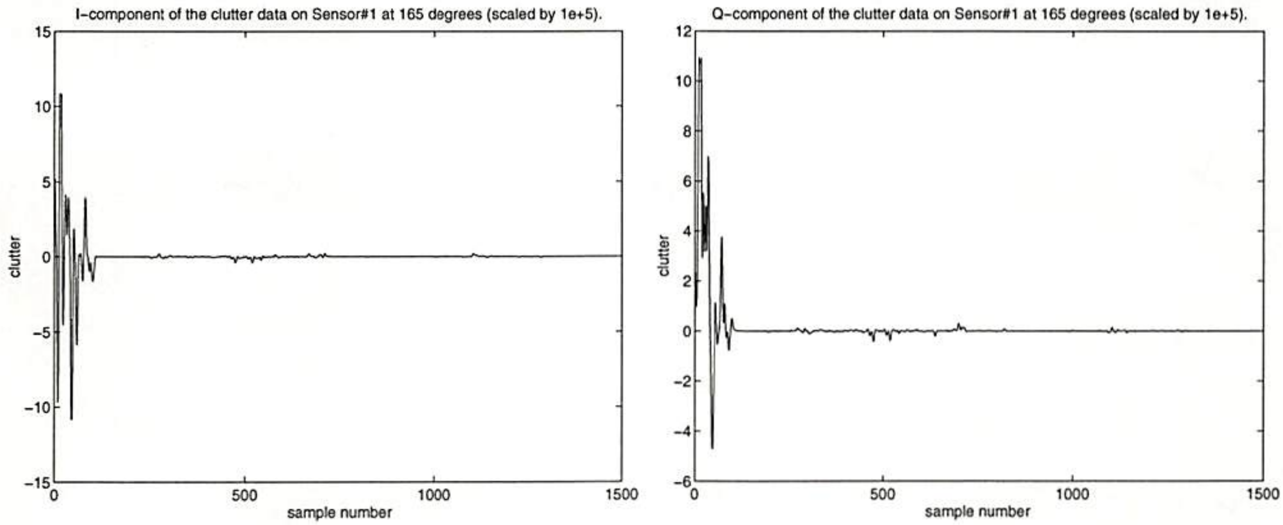

Figure 23: Measured I/Q-components of radar clutter: Azimuth: 165°, estimated mean: $-0.0046 + j0.1344$, estimated α: 1.5249, γ: 0.031.

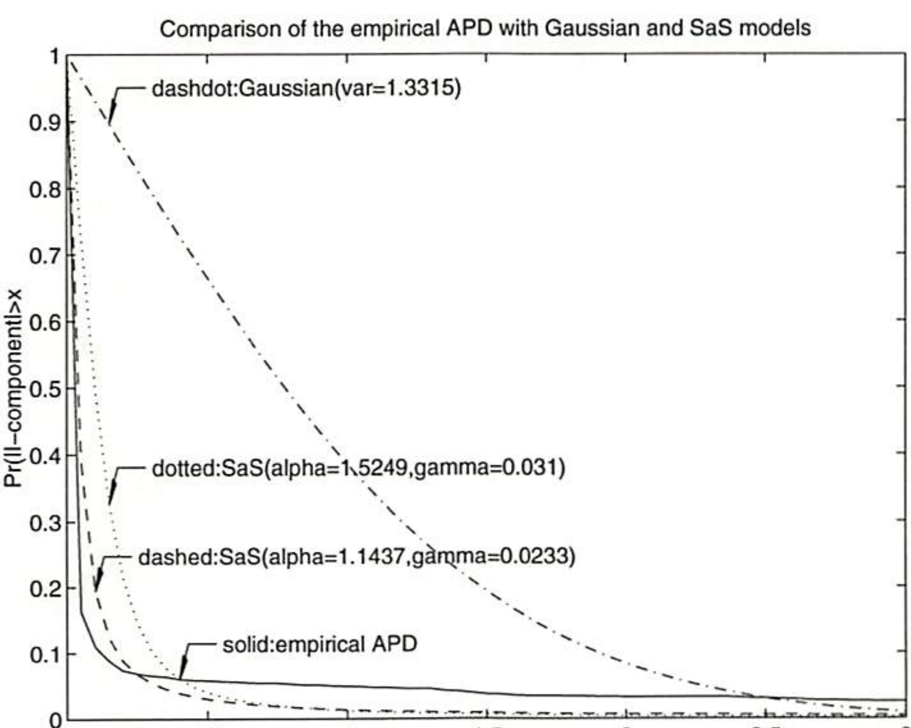

Figure 24: Comparison of the empirical, SαS, and Gaussian amplitude probability distributions

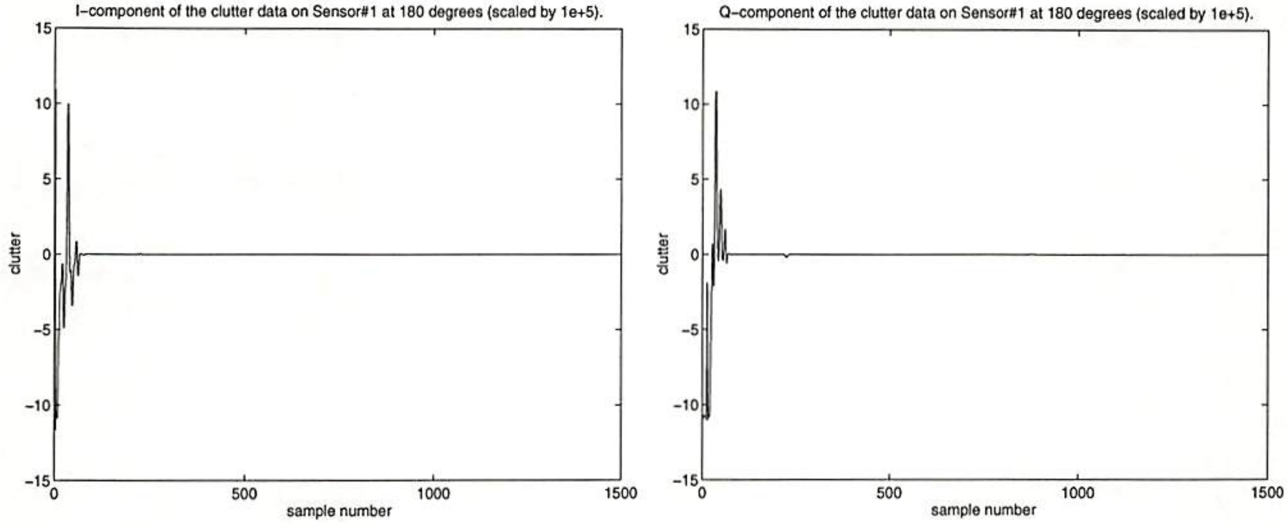

Figure 25: Measured I/Q-components of radar clutter: Azimuth: 180°, estimated mean: $-0.0734 - j0.0939$, estimated α: 1.7156, γ: 0.0155.

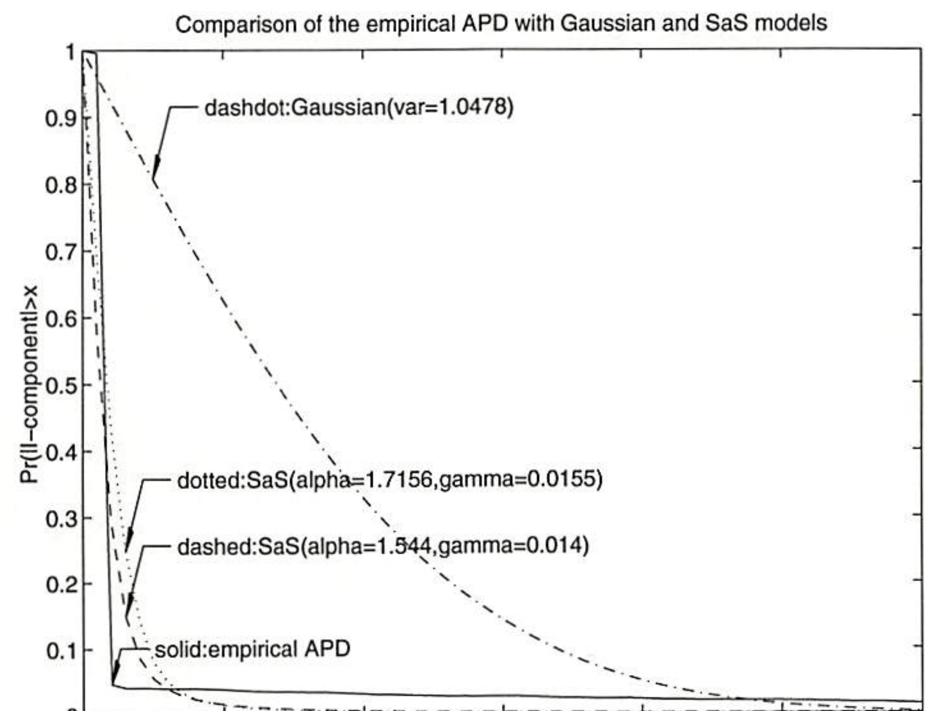

Figure 26: Comparison of the empirical, SαS, and Gaussian amplitude probability distributions

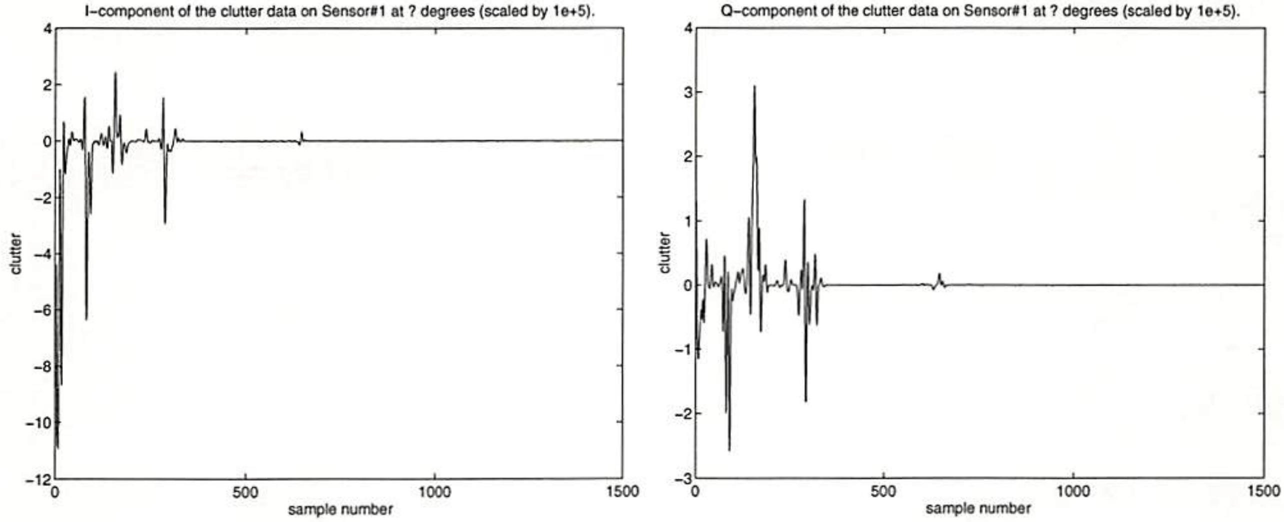

Figure 27: Measured I/Q-components of radar clutter: Azimuth: 195°, estimated mean: $-0.1158 + j0.0059$, estimated α: 1.6606, γ: 0.0195.

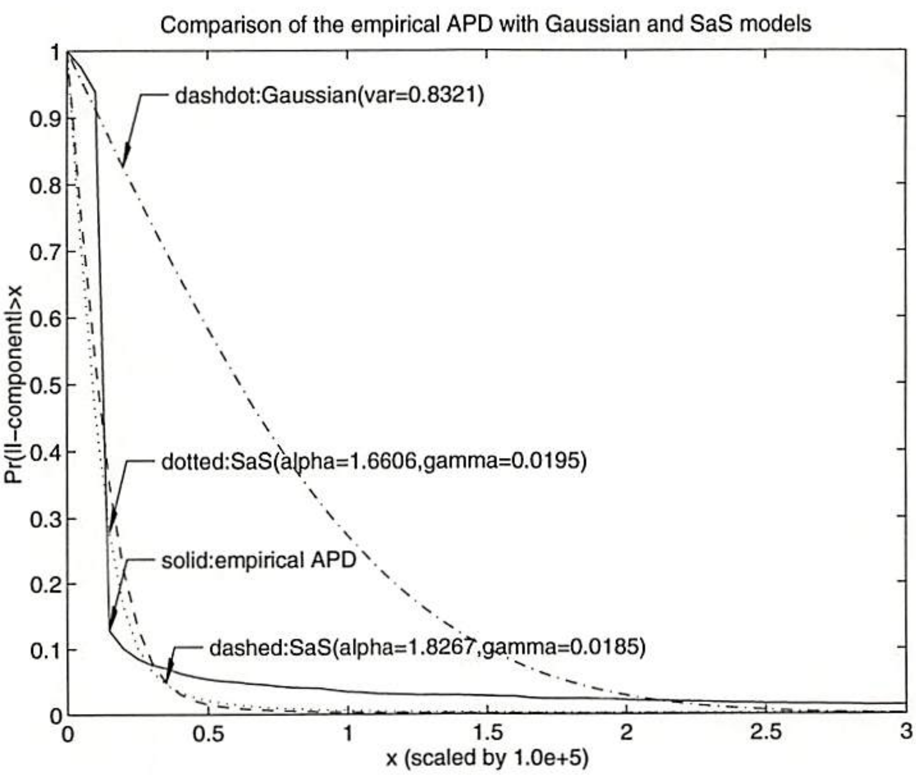

Figure 28: Comparison of the empirical APD with Gaussian and SαS models

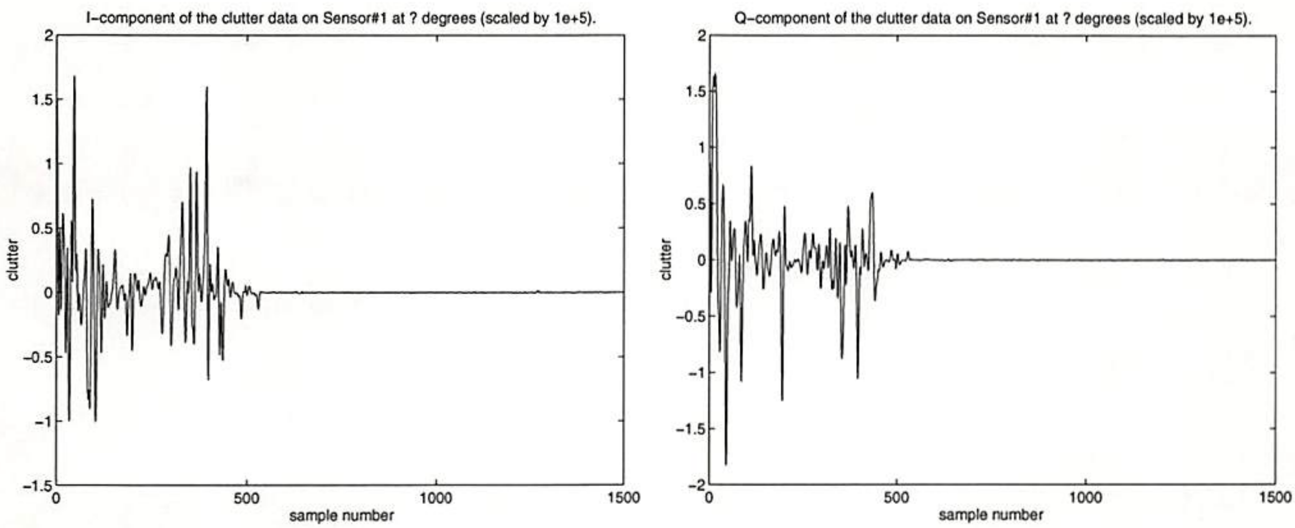

Figure 29: Measured I/Q-components of radar clutter: Azimuth: 210°, estimated mean: $0.014 + j0.0025$, estimated α: 0.8981, γ: 0.0254.

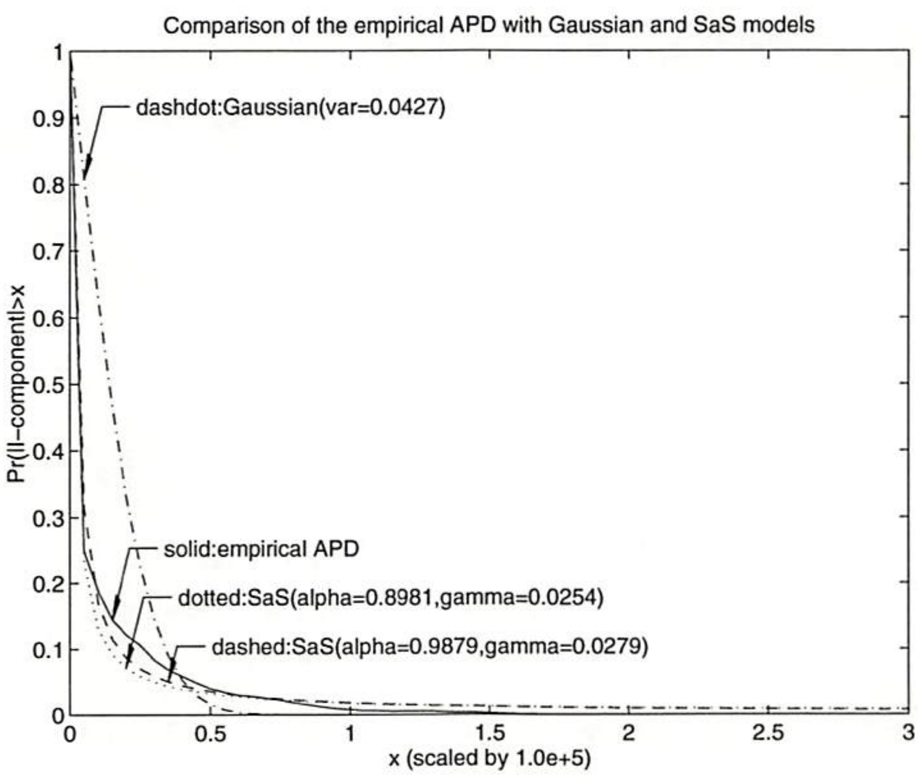

Figure 30: Comparison of the empirical APD with Gaussian and SαS models

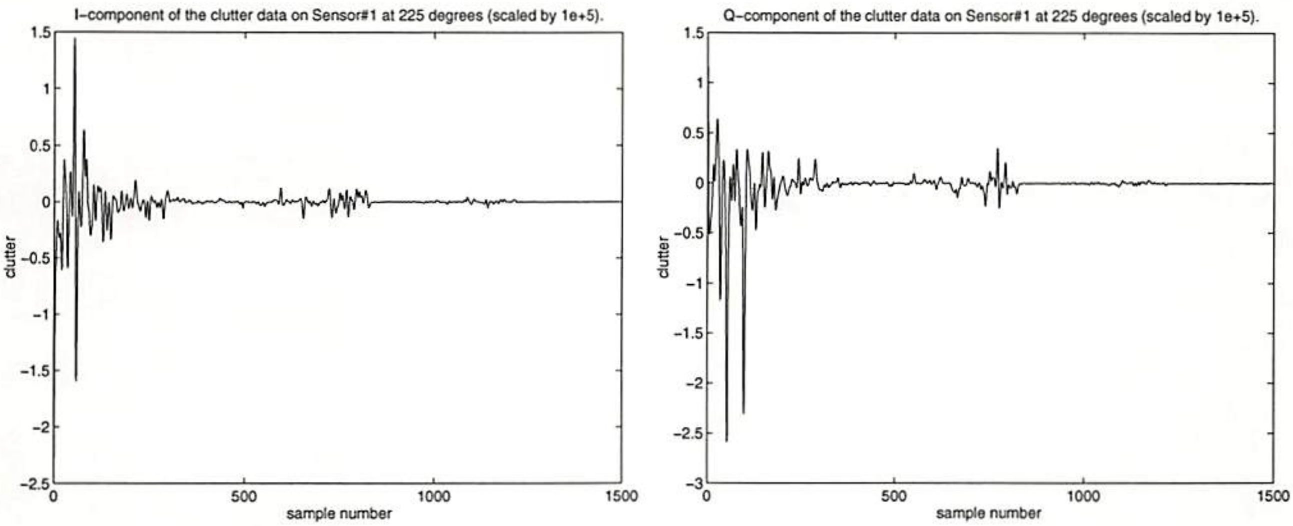

Figure 31: Measured I/Q-components of radar clutter: Azimuth: 225°, estimated mean: $-0.0099 - j0.0248$, estimated α: 1.322, γ: 0.0079.

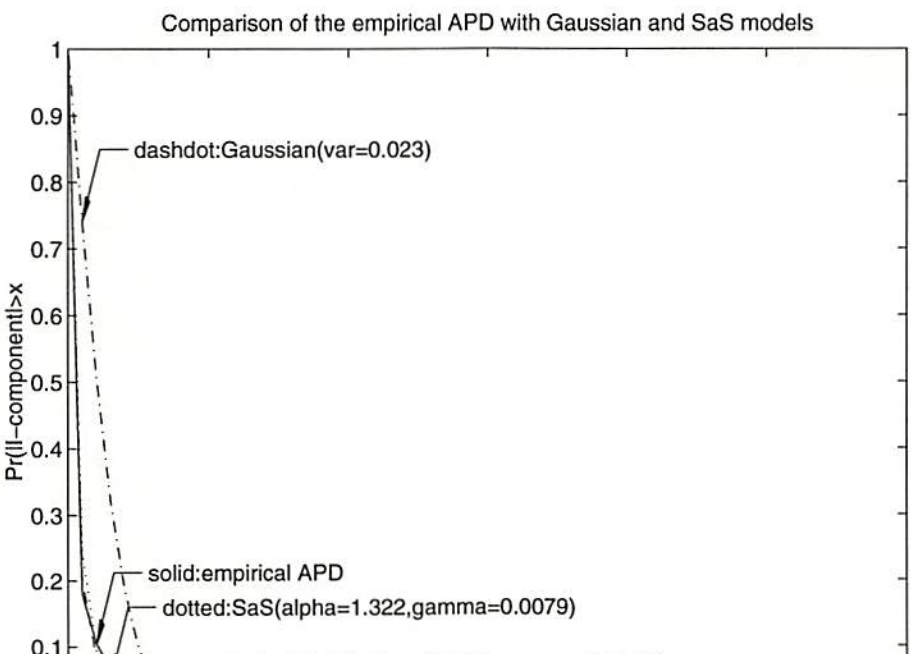

Figure 32: Comparison of the empirical APD with Gaussian and SαS models

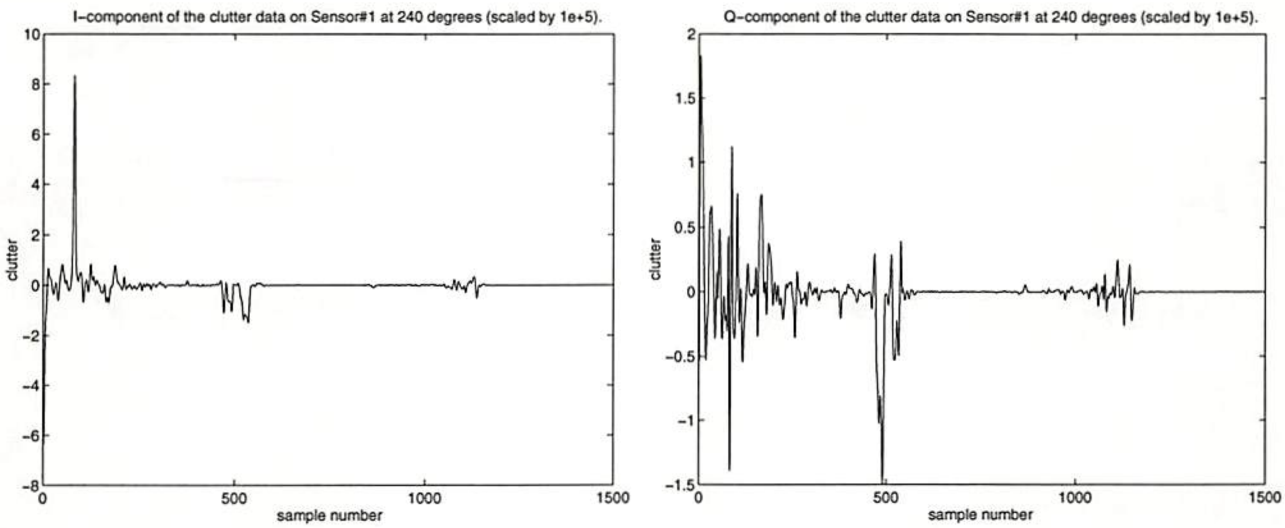

Figure 33: Measured I/Q-components of radar clutter: Azimuth: 240°, estimated mean: $-0.0092 - j0.007$, estimated α: 0.8358, γ: 0.0337.

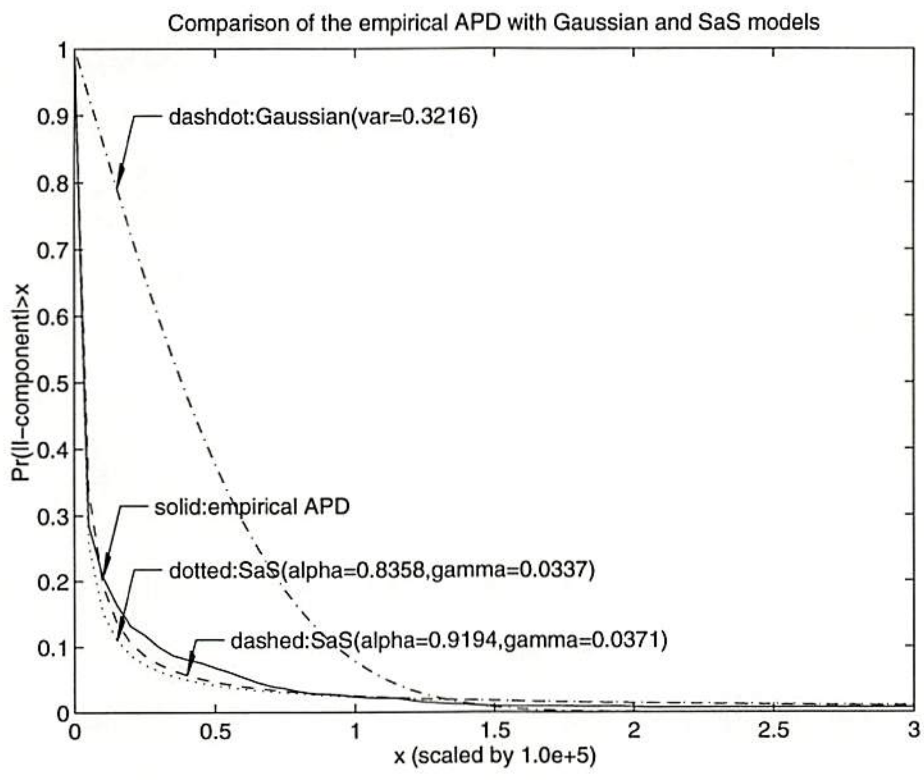

Figure 34: Comparison of the empirical APD with Gaussian and SαS models

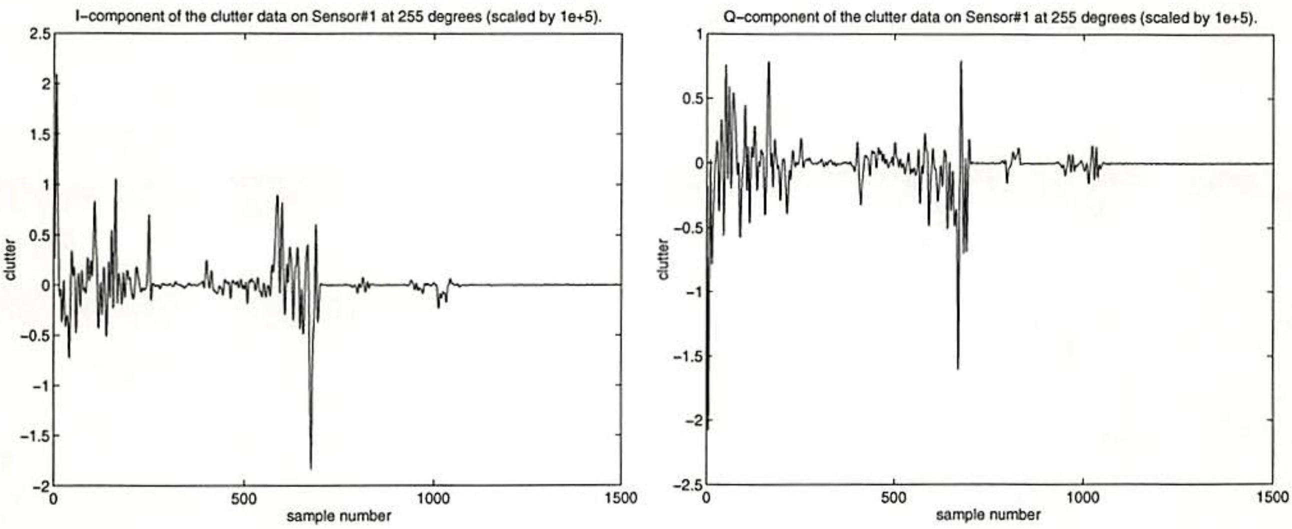

Figure 35: Measured I/Q-components of radar clutter: Azimuth: 255°, estimated mean: $0.0085 - \jmath 0.0215$, estimated α: 1.0626, γ: 0.0234.

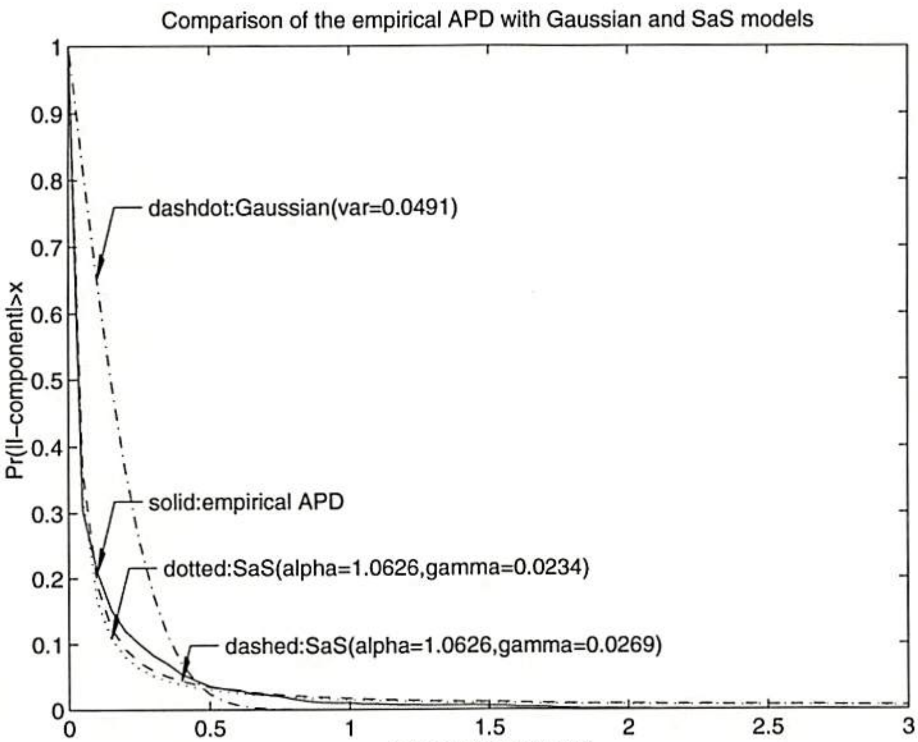

Figure 36: Comparison of the empirical APD with Gaussian and SαS models

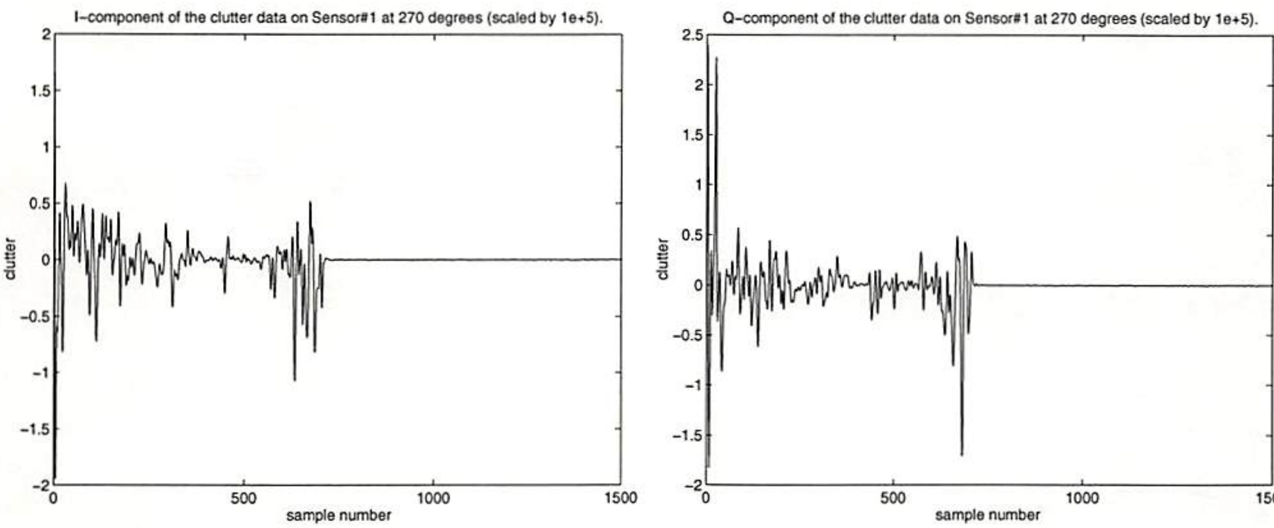

Figure 37: Measured I/Q-components of radar clutter: Azimuth: 270°, estimated mean: $-0.0085 - j0.0055$, estimated α: 0.8239, γ: 0.0327.

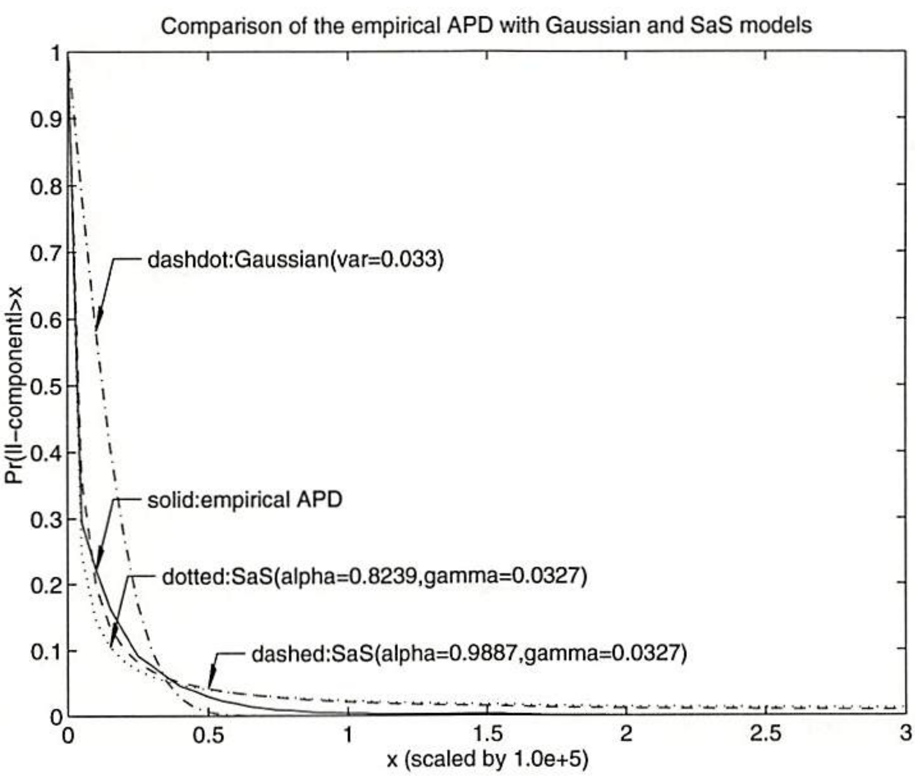

Figure 38: Comparison of the empirical APD with Gaussian and SαS models

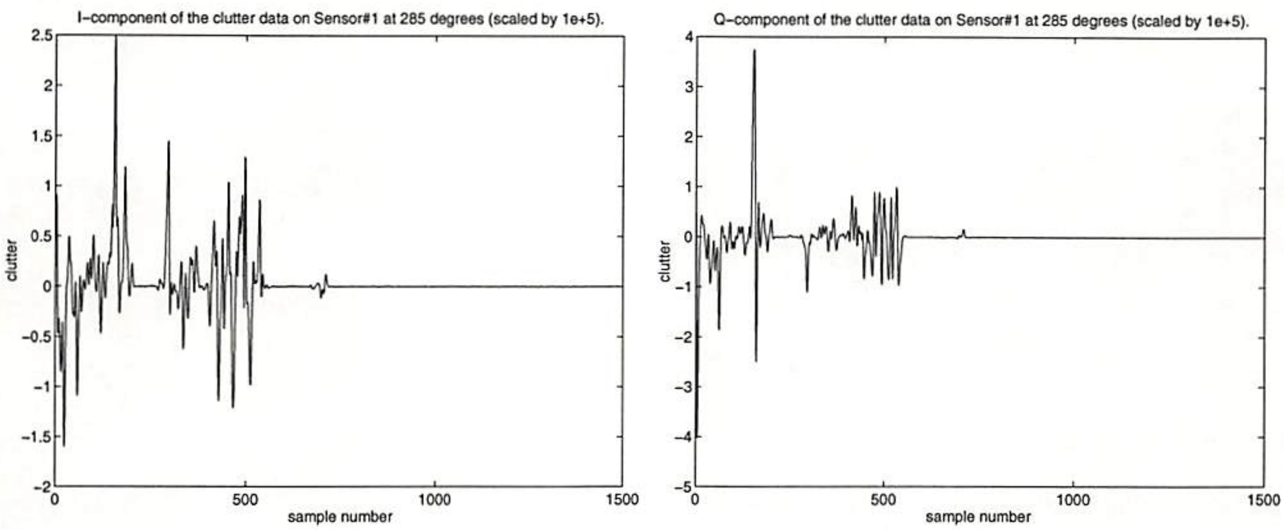

Figure 39: Measured I/Q-components of radar clutter: Azimuth: 285°, estimated mean: $0.0239 - j0.0141$, estimated α: 0.9738, γ: 0.0336.

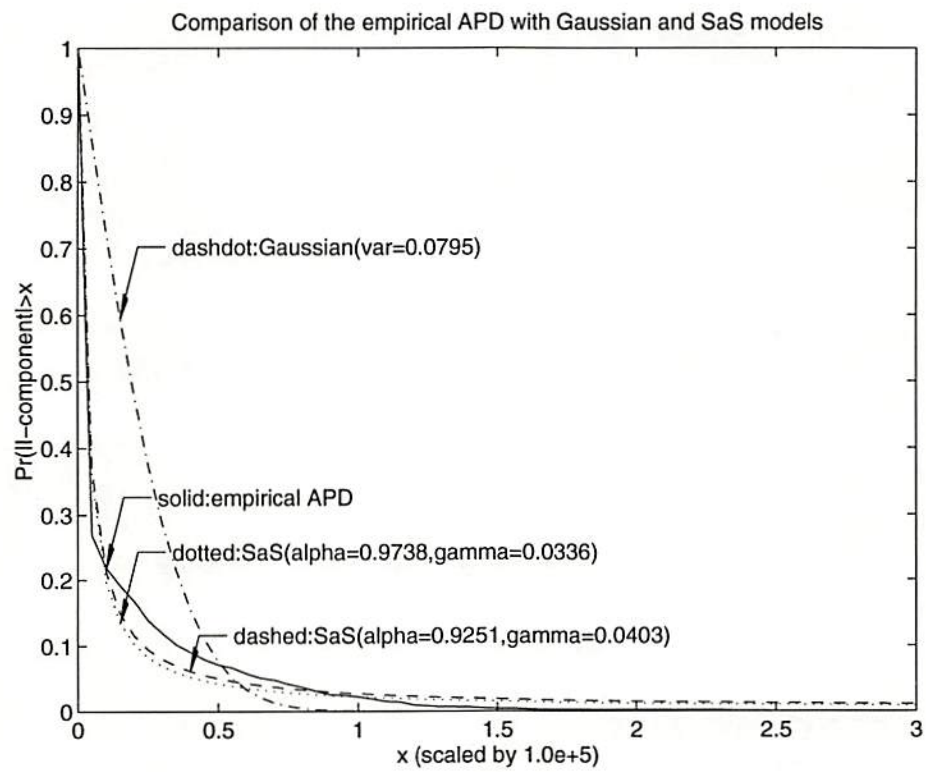

Figure 40: Comparison of the empirical APD with Gaussian and SαS models

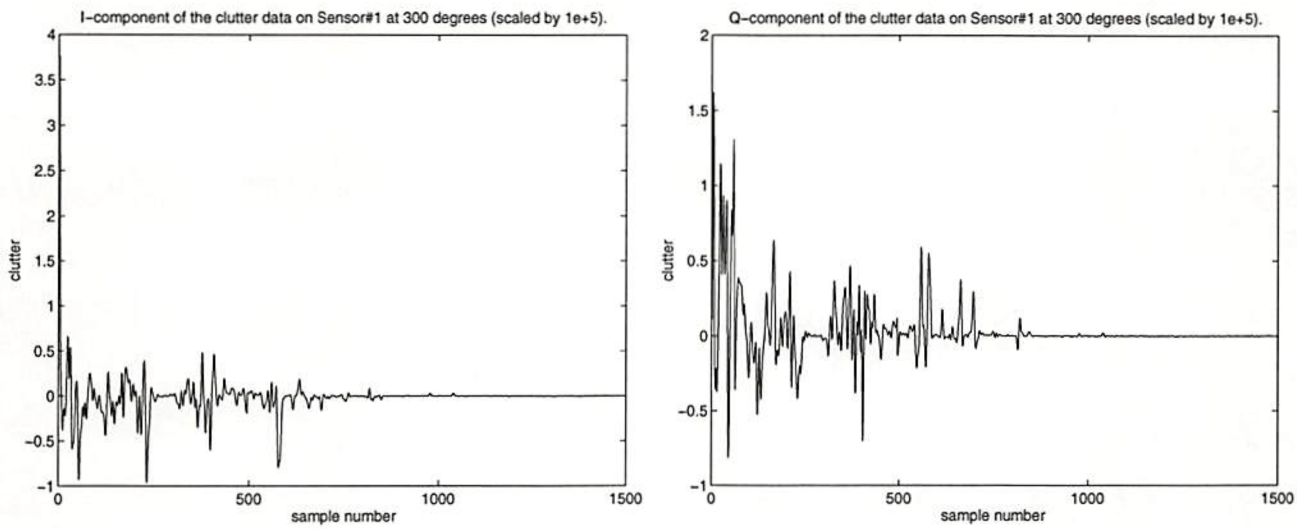

Figure 41: Measured I/Q-components of radar clutter: Azimuth: 300°, estimated mean: $-0.0137 + j0.0308$, estimated α: 1.2517, γ: 0.0159.

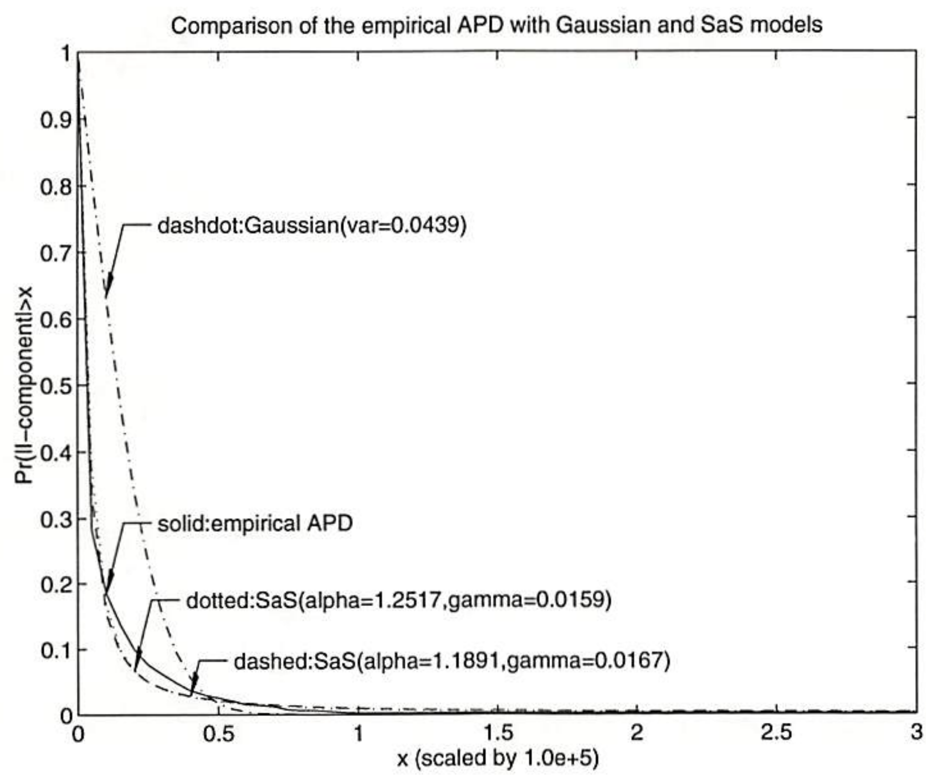

Figure 42: Comparison of the empirical APD with Gaussian and SαS models

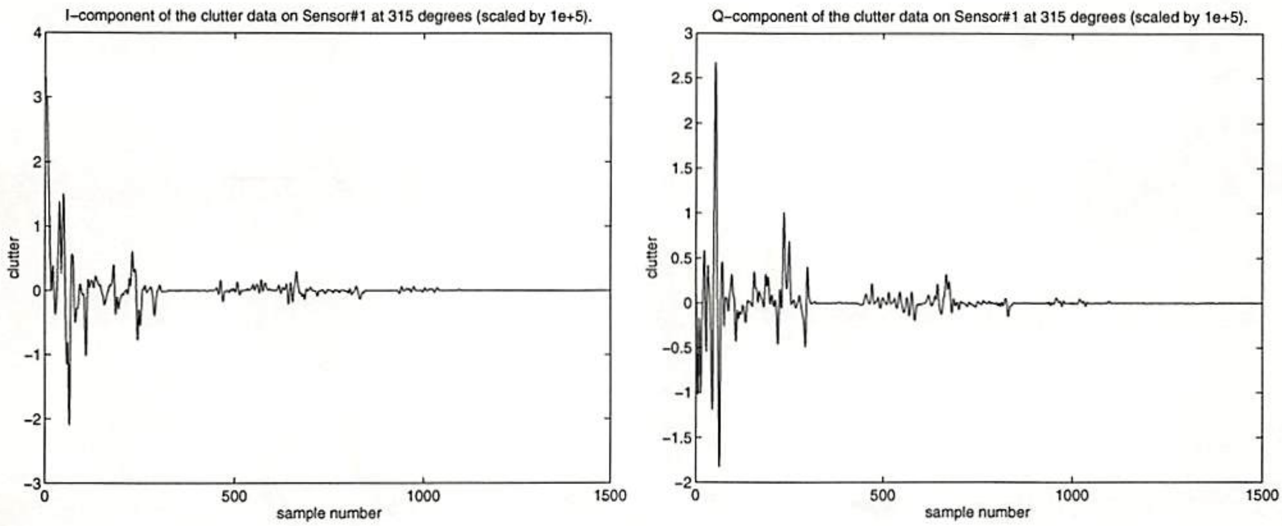

Figure 43: Measured I/Q-components of radar clutter: Azimuth: 315°, estimated mean: $0.017 + j0.0079$, estimated α: 1.0304, γ: 0.0193.

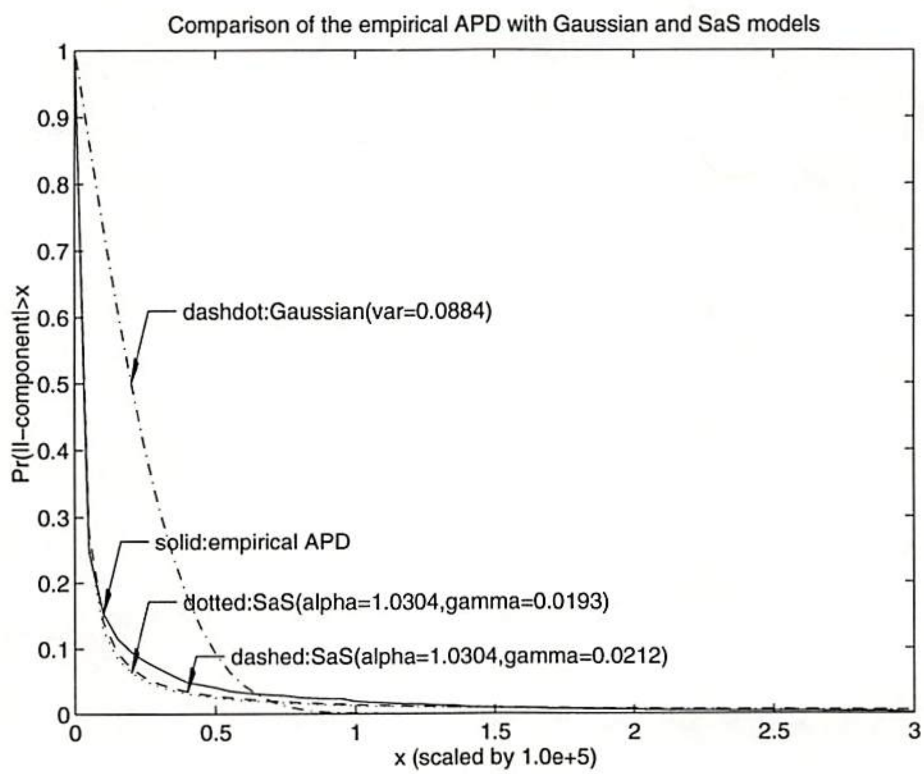

Figure 44: Comparison of the empirical APD with Gaussian and SαS models

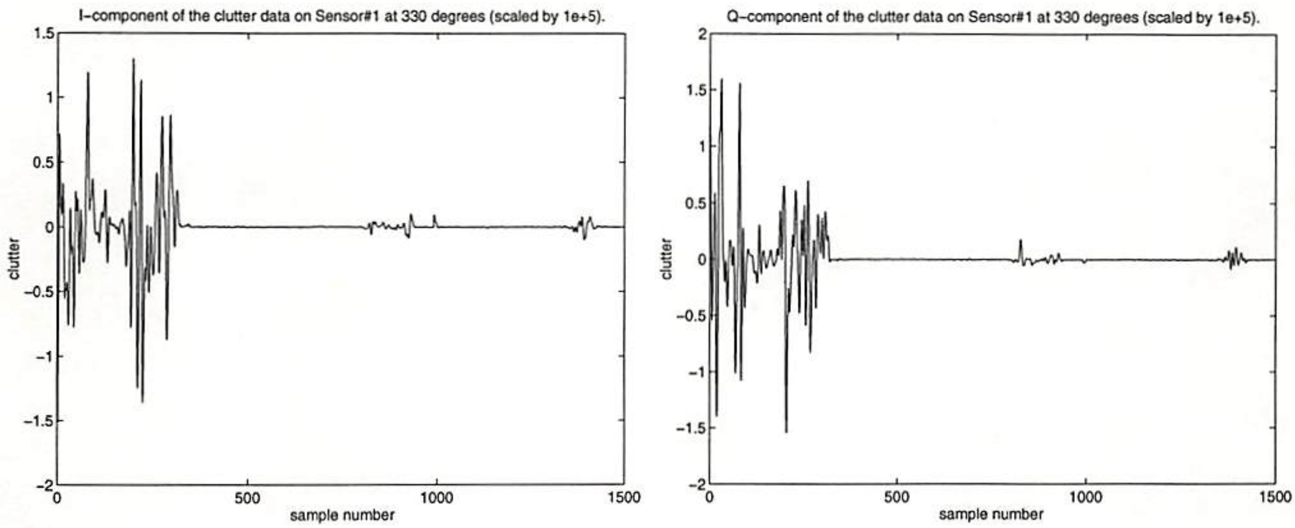

Figure 45: Measured I/Q-components of radar clutter: Azimuth: 330°, estimated mean: $-0.0015 + j0.0063$, estimated α: 0.7749, γ: 0.0239.

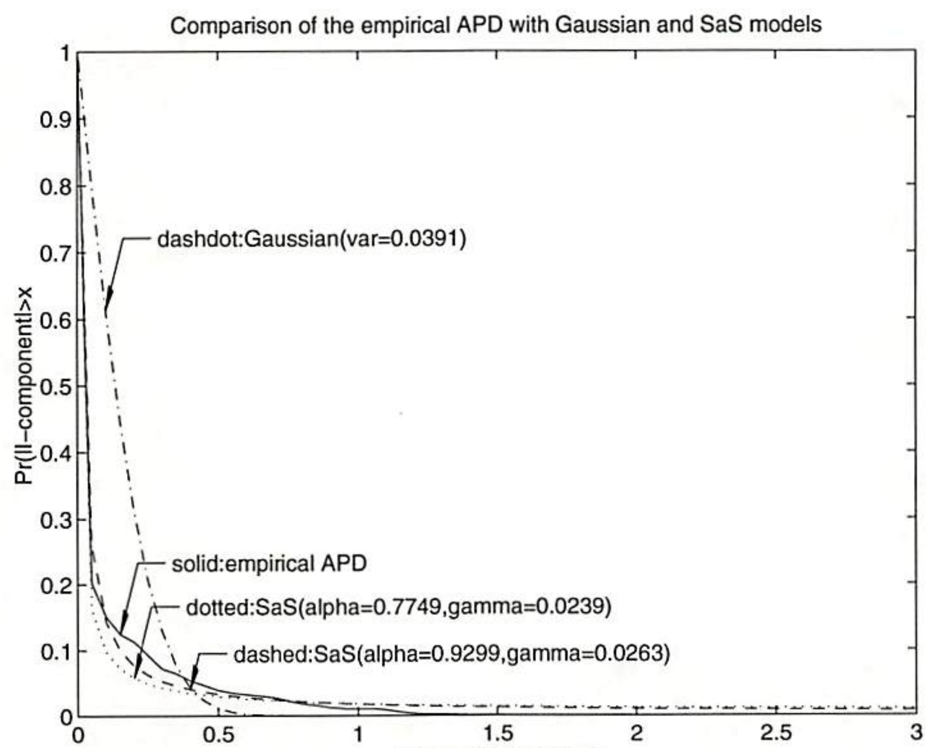

Figure 46: Comparison of the empirical APD with Gaussian and SαS models

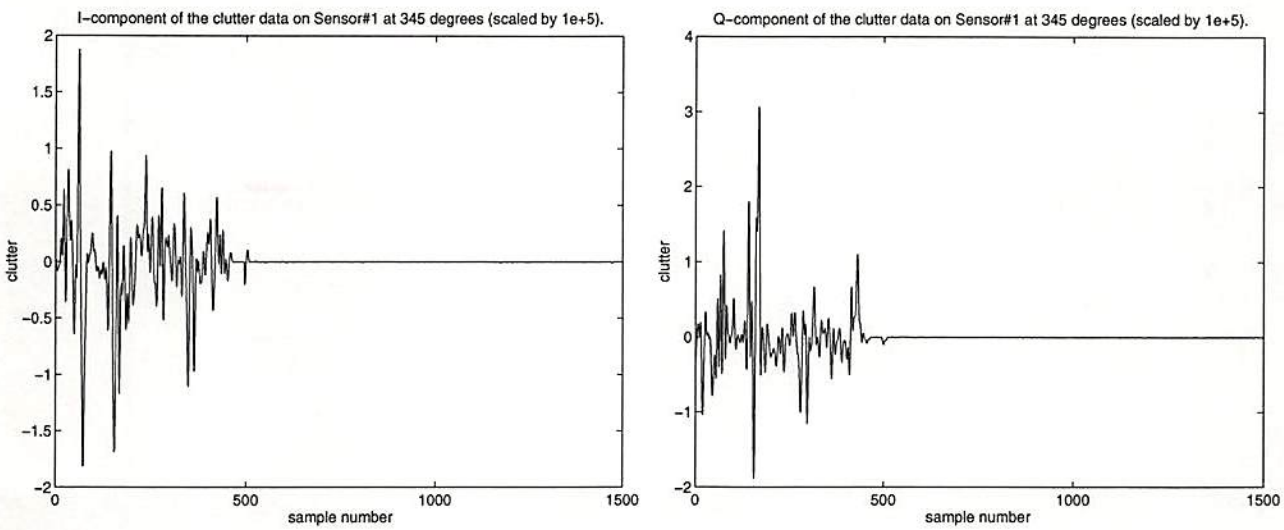

Figure 47: Measured I/Q-components of radar clutter: Azimuth: 345°, estimated mean: $-0.0097 + j0.0051$, estimated α: 0.7785, γ: 0.0345.

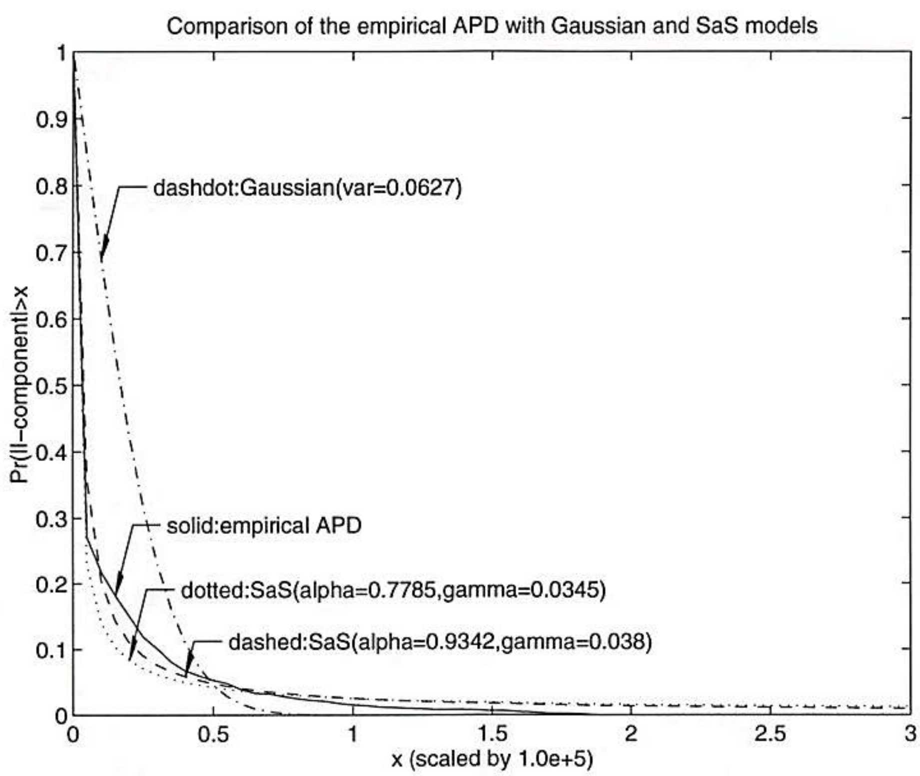

Figure 48: Comparison of the empirical APD with Gaussian and SαS models

Our experiments show SαS distribution is superior to the traditional Gaussian distribution for modeling the actual radar clutter data.

4 Conclusion

In this report, we introduced new methods for parameter estimation of SαS processes and argued that stable laws could approximate impulsive processes such as radar clutter environments accurately. Extensive experiments were conducted using real clutter data. These experiments showed stable distributions were very close to the empirical densities of the clutter data.

References

[1] X. Ma and C. L. Nikias, "Parameter Estimation and Blind Channel Identification for Impulsive Signal Environments," *IEEE Trans. Signal Processing*, Dec. 1995. To Appear.

[2] C. L. Nikias and M. Shao, *Signal Processing with Alpha-Stable Distributions and Applications*, New York, NY: John Wiley & Sons, 1995.

[3] M. Shao and C. L. Nikias, "Signal Processing with Fractional Lower Order Moments: Stable Processes and Their Applications," *IEEE Proc.*, July 1993.

[4] V. Zolotarev, *One-dimensional Stable Distributions*, Providence, RI: American Mathematical Society, 1986.

[5] V. M. Zolotarev, "Integral Transformations of Distributions and Estimates of Parameters of Multidimensional Spherically Symmetric Stable Laws," in *Contribution to Probability:*

A Collection of Papers Dedicated to Eugene Lukacs (J. Gani and V. K. Rohatgi, eds.), pp. 283–305, Academic Press, 1981.